PROCESSING AND CHARACTERIZATION OF SCANDIUM ADDED A356 CAST ALLOY

A Thesis Submitted to
the Graduate School of Engineering and Sciences of
İzmir Institute of Technology
in Partial Fulfillment of the Requirements for the Degree of

MASTER OF SCIENCE

in Mechanical Engineering

by

Cezmi ÖNER

October 2021

İZMİR

ABSTRACT

PROCESSING AND CHARACTERIZATION OF SCANDIUM ADDED A356 CAST ALLOY

As a result of today's rapid technological developments and the rapid consumption of reserves in the world, the search for alternative materials has started. One of the biggest examples of this is wheel alloy. Ti_5B_1, one of the additives of the A356 Al alloy that is generally used in automobile wheels, allows to reduce the grain size in the alloy. In the event of depletion of possible Ti_5B_1 resources, there will be a need to use alternative materials instead. Based on this purpose, materials that can be used instead of Ti_5B_1 were examined. Scandium (Sc) as a rare earth element was found to be the least studied element with A356. A number of Sc-based studies with other aluminum alloys were reported and it was decided to work with this element for A356 alloy.

In the thesis, the effect of Sc adjunction on the mechanical properties of A356 aluminum alloy after the permanent die casting process was investigated. Sc added to the A356 alloy at a ratio of 0.2, 0.4 and 0.6 weight percent, respectively. Optical microscopy (OM), Scanning electron microscopy (SEM) with energy dispersive spectroscopy (EDS) were used for the microstructural analyses in this study. According to the experiments and results obtained in this study, it was observed that Sc can significantly increase the mechanical properties of the A356 alloy in terms of tensile strength and hardness values. Overall, it was found that the addition of 0.2 wt.% Sc to the A356 alloy could achieve a maximum tensile strength of 258.31 MPa compared to 242.54 MPa for the reference sample without Sc. No significant improvement in tensile strength results was observed when more than 0.2 wt.% Sc was added to the alloy. As for the hardness, the sample containing 0.2 wt.% Sc reached a maximum Brinell hardness of 75.01 HB compared to 77.58 HB for the unmodified sample. As a result, the amount of porosity increased with Sc added to the alloy, and an increase in dendrite arm lengths occurred. Due to this length in the arms, a decrease in fracture toughness occurred. In addition, there was no significant improvement in hardness.

ÖZET

SKANDİUM KATKILI A356 DÖKÜM ALAŞIM PROSESİ VE KARAKTERİZASYONU

Günümüzün hızlı teknolojik gelişmeleri ve dünyadaki rezervlerin hızla tüketilmesi sonucunda alternatif malzeme arayışları başlamıştır. Bunun en büyük örneklerinden biri jant alaşımıdır. Otomobil jantlarında sıkça kullanılan A356 alüminyum alaşımının katkı maddelerinden biri olan Ti_5B1, alaşımdaki tane boyutunun rafine edilmesini sağlar. Olası Ti_5B_1 kaynaklarının tükenmesi durumunda bunun yerine alternatif malzemelerin kullanılmasına ihtiyaç duyulabilir. Bu amaçtan yola çıkılarak Ti_5B_1 yerine kullanılabilecek malzemeler araştırılmış ve listelenmiştir. Scandium (Sc), A356 ile en az çalışılan element olarak göze çarpmaktadır . Diğer alüminyum alaşımları ile yapılan Sc çalışmaları incelenmiş ve bu element ile çalışılmasına karar verilmiştir.

Bu tezde, kokil döküm işleminden sonra A356 alüminyum alaşımına skandiyum (Sc) ilavesinin mekanik özelliklere etkisi incelenmiştir. Skandiyum, A356 alaşımına sırası ile 0.2, 0.4 ve 0.6 ağırlık yüzdelerinde ilave edilmiştir. Bu çalışmada, malzemelerin mikroyapı incelemelerinde optik mikroskopi (OM) ve enerji dağılımlı spektroskopi (EDS) ile taramalı elektron mikroskobu (SEM) kullanılmıştır. Bu çalışmada yapılan deneyler ve elde edilen sonuçlara göre Sc'un A356 alaşımının mekanik özelliklerini çekme mukavemeti açısından önemli ölçüde artırabildiği gözlemlenmiştir. Genel olarak, A356 alaşımına ağırlıkça %0.2 Sc ilavesinin, Sc içermeyen numune için 242.54 MPa'ya kıyasla 258.31 MPa'lık maksimum çekme mukavemetine ulaşabildiği gözlemlenmiştir. Alaşıma ağırlıkça % 0.2 'den fazla Sc eklendiğinde çekme mukavemetinde önemli bir gelişme görülmemiştir. Sertlik açısından, ağırlıkça %0.2 Sc içeren numune, modifiye edilmemiş numunenin sahip olduğu 77.58 HB değerine kıyasla 75.01 HB maksimum Brinell sertlik değerine ulaşmıştır. Sonuç olarak, alaşıma eklenen Sc ile porozite miktarı arttı, dendirit kol uzunluklarında artış meydana geldi. Kollarda oluşan bu uzunluk nedeni ile kırılma tokluğunda düşüş meydana gelmiştir. Bunlara ek olarak sertlikte de önemli bir gelişme kaydedilmemiştir.

TABLE OF CONTENTS

LIST OF FIGURES

Figure **Page**

Figure **Page**

LIST OF TABLES

Table **Page**

CHAPTER 1

INTRODUCTION

With the growing need for lightweight parts, improving strength and ductility of light alloys such as aluminum (Al) and magnesium (Mg) has become of paramount importance in industries [1]. In addition to these features, the factors such as making excellent castings with a good combination of strength and ductility, improved wear and resistance to corrosion are also demanded in aerospace and automotive industries., In line with these demands, the use of Al–Silicon (Si) Mg alloys has become widespread [1,2].

One of the most common and familiar methods for strengthening Al alloys is to use micro-alloy additions with fine dispersion of precipitates. Sc is known to be one of the most effective micro-alloy reinforcing/ strengthening elements for Al alloys [3], and this approach was patented by Lowell A. Willey Lower Burrell in 1971 [4]. Sc as one of the rare-earth elements strengthens Al and its alloys in three different ways, these are: (1) grain refining, (2) precipitation hardening/recrystallization inhibition, and (3) grain growth [5]. Despite its advantages, Sc has historically been limited to industrial use due to its high cost and low availability. However, it is expected to be a reliable alternative for industrial use in the next decade with the help of its worldwide known and usage by more researchers and decreasing production cost with new efficient extraction technologies [1].

Niranjan and Lakshminarayanan [6] and Suresh et al. [7] obtained an enhance in wear resistance in Al-TiB_2 composite by using TiB_2 content. Kumar et al. [8] studied the effect of 5-10 wt.% TiB_2 respectively, in Al–7Si alloy and reported nearly 50% reduction in wear rate and nearly 40% increase in tensile property for 10 wt.% TiB_2 content. Mandal et al. [9] studied the wear behavior of A356–5/10 wt.%TiB_2 composites and showed that with the TiB_2 content the wear resistance improves significantly. In the study conducted by Røyset and Ryum [10], it was observed that adding a small amount of Zirconium (Zr) with the Sc element into results in an increase in recrystallization resistance. In their study, the aluminum alloys with 0.2 5% Sc and 0.08% Zr by weight addition were cold worked, resisted recrystallization at 520 °C for 8 hours and did not show recrystallization up to about 600 ° C. Another study with the Sc element was

conducted by Prukkanon et al. [11]. In this study, it was observed that modification with Sc did not decrease the fluidity of the melt. The fluidity of the A356 samples modified with 0.2 wt.% Sc, 0.4 wt.% Sc and also 0.2 wt.% Zr increased with increasing temperature. The scandium and Sc - Zr additions were also noted to significantly reduce the grain size of the cast aluminum samples. The fluidity of these samples with finer grain size is higher than that of the unmodified samples. To summarize, in that study, the fluidity tests were applied on the Sc modified A356 alloy, and it was observed that the addition of 0.2% and 0.4% by weight increased the fluidity more than 40%. Pramod et al. [12] investigated the effect of Sc addition on the grain refinement, modification of eutectic Si, mechanical and wear properties of A356–10 wt.% TiB_2 in-situ composite. This adjunct resulted in reduction of α-Al the secondary dendrite arms spacing (SDAS) and modification of eutectic Si. Compared to that of A356 alloy, hardness values of A356-0.4 wt.% Sc alloy and A356–10 wt.% TiB_2 composite with 0.4 wt.% Sc increased by 20% and 45%, respectively.

In this thesis, it is aimed to use Sc as a grain refiner and to investigate the other effects of Sc addition.

CHAPTER 2

LITERATURE REVIEW

2.1. Aluminum and Aluminum Alloys

Aluminum is an important element found in the earth in different mineralogical forms such as Al_2O_3, bauxite, corundum or bonded with silica and, alumina silicates. The metallurgical process of aluminum is a difficult process due to its affinity for oxygen and its tendency to form the oxide layer. Bayer and Hall-Heroult processes are the most widely used processes for aluminum production [13,14]. In the un-alloyed state, pure aluminum is a relatively soft material with a yield strength of 34.5 MPa, a tensile strength of 90 MPa and a density of about 2.7 g / cm^3 [15]. Silicon (Si), Magnesium (Mg), Copper (Cu), Zinc (Zn), Manganese (Mn) and Nickel (Ni) are used to produce different types of aluminum alloys. All these elements are added to pure aluminum to improve mechanical properties.

Effect of alloying elements on aluminum are as follows:

Copper (Cu): Copper greatly improves strength and hardness in cast alloys and heat-treated alloys. The solubility of copper in aluminum is 0.5 wt.% at room temperature and 5.65 wt.% at 548 ° C eutectic temperature. With the addition of Cu up to 5.5 wt.%, strength increases, and ductility decreases in Al-Cu alloys. Mechanical properties decrease with the addition of higher amounts of Cu. It was reported that Al-Cu alloy with the best casting properties contains 8 wt.% Cu [16,17].

Iron (Fe): Iron increases hot tear resistance and reduces the tendency of liquid metal to stick to the mold in castings using metal molds. Iron found in Al alloys at ratios over 1,3 wt.% decreases the ductility. Another negative effect of high iron ratio is that the grain structure of the alloy leads to coarsening [17].

Manganese (Mn): The addition of 0.5 wt.% Mn in Al alloys increases the hardness and ductility [17].

Zinc (Zn): Zn is rarely used in aluminum casting alloys as it causes hot tearing. The most important effect of Zn is that it increases the strength and machinability of the alloy. It is preferred due to its natural aging feature. It also increases the weldability [17].

Magnesium (Mg): The Mg ratio in commonly used Al-Mg alloys is between 4-10 wt.%. The addition of Mg provides high strength, high corrosion resistance and high welding ability to the Al alloys. Especially in Al-Mg alloys used in the maritime industry, high mechanical properties and fine-grained structure are preferred [19].

Silicon (Si): The addition of Si to pure aluminum significantly improves its fluidity, and hot tear resistance properties. Due to these properties, the most widely used aluminum alloys in the industry are Al-Si alloys. Al-Si alloys containing 7-12 wt.% silicon is employed under conditions that require high strength and high temperature abrasion resistance [19].

Scandium (Sc): Sc is a suitable additive (as an alloying element) to improve the weldability, heat resistance and creep properties of high strength alloys. Also, Sc addition causes grain refinement as it significantly affects grain development and sub-grain size. Studies have shown that the addition of Sc transforms the growth morphology of dendrites in the alloy into fine spherical grains [20].

2.2. Al-Si-Mg Alloys (A356)

Al-Si alloys are used in defense industry, aviation, and automotive sectors due to their lightness, high strength, high thermal conductivity, and low thermal expansion properties. In Al-Si-Mg alloys; while Si increases the casting capability, Mg improves the yield and tensile strength. As depicted in from Figure 2.1 Al alloys containing less than 14 wt.% Si are called hypo-eutectic, while Al alloys containing 14 wt.% or more Si are called hyper-eutectic. The increase in strength and ductility of Al-Si alloys, especially in alloys containing high amounts of silicon, is achieved by the modification at Al-Si eutectic point [21,22].

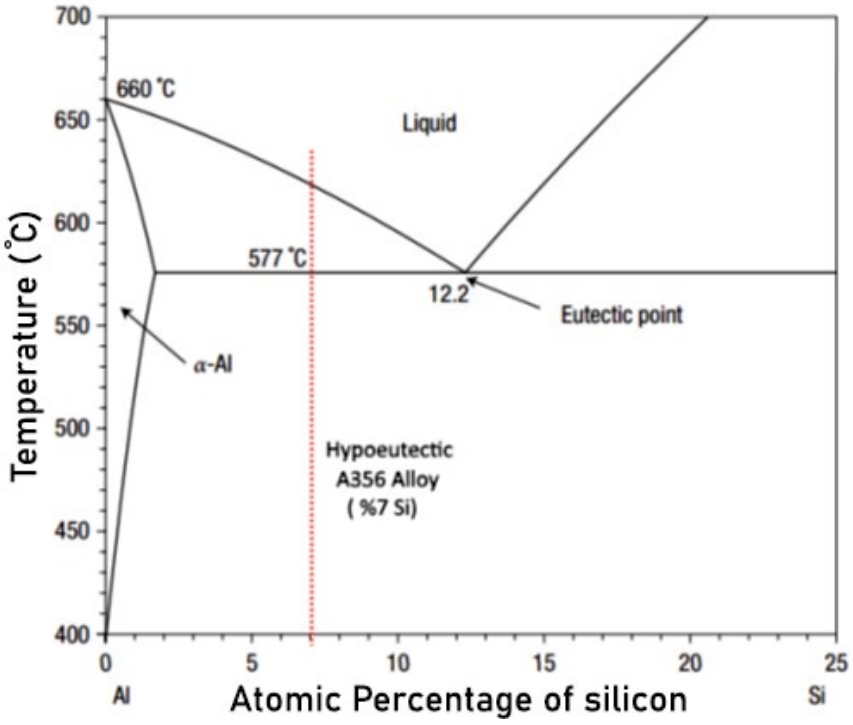

Figure 2.1. Al–Si binary phase diagram [23]

Mg is the basic solid solution booster for Al - Si alloy (to form Al - Si - Mg alloys) and its addition leads to an increase in precipitation hardening resulting in higher yield strength in these alloys [24].

The most important and widely used alloy among Al-Si-Mg alloys is “Hypoeutectic cast” A356 alloy. Since the A356 alloy contains 7% Si by weight, it is a material with high castability properties. Approximately 0.35 wt.% Mg in its composition enables this alloy to be strengthened by aging [25,26]. The composition of the A356 alloy is given in Table 2.1.

Table 2.1. Chemical composition of A356 alloy (wt.%)

Al	Si	Cu	Fe	Mn	Mg	Zn	Ti
Bal.	6.5-7.5	0.2 0	0.2 0	0.10	0.25-0.45	0.10	0.2 0

2.3. Scandium Master Alloy

Scandium (Sc) has an atomic number of 21. Firstly, it was named as “Eka-boron” [27]. It is classified as a rare earth element along with “yttrium” and “lanthanides”. It was discovered in 1879 by Lars Fredrik Nilsson through spectral analysis of euxenite and gadolinite minerals from Scandinavia [28]. Sc is commonly found in deposits of rare earth and uranium compounds, but only a few mines are mined worldwide. It took the 1970s to understand the effects of Sc on Al /Al alloys. Due to its new discovery and the difficult stages, it contained, it was used in certain private sectors in those years [29]. The global Scandium oxide trade is 15-20 tons per year [30].

In this thesis, 7 kilograms of aluminum-based master alloy containing 2% Sc from KBM AFFILIPS was used. Figure 2.2 and Figure 2.3 show the 2% Sc-Al master alloy and the $AlSc_2$ waffle ingot phase as indicated by the arrow in the 30μm matrix, respectively. Chemical composition of 2% Sc, Al master alloy shown in Table 2.2.

Figure 2.2. 2% Sc, balance Al master alloy

Table 2.2 Al-2 wt.% Sc master alloy

Element	Sc	Si	Fe	Mg	Other
wt.%	1.9-2.2	0.1	0.1	0.2	0.15

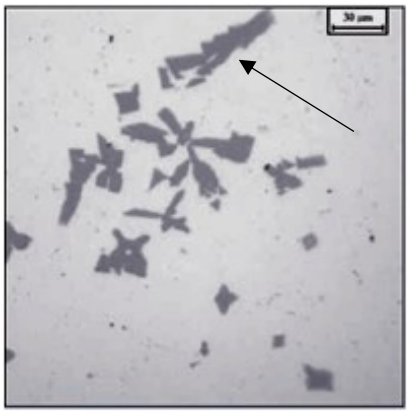

Figure 2.3. AlSc2% waffle ingot phase in matrix

2.3.1. Application Area of Al-Sc Alloys

Because of high price and lack of abundance of Sc element, current use of these alloys are restricted despite of all the improvements and benefits by addition of Sc to Al alloys. For this reason, Al-Sc alloys are used in particular applications or for Scientific research [10].

These applications are as follows:

•Aerospace industry such as bulk heads, heat shields, seat tracks, wheels, running gears, fuel, and exhaust systems. [31]

•Bicycle frames, baseball bats, handguns frames, golf clubs tent poles and lacrosse sticks [3,10,31].

•In the automotive industry such as body frame and crash management systems (due to high strength extrusions) [31,32]

Considering the usage areas of Scandium, one of the most important application areas is metallurgy. It is known as an effective alloying element. When Scandium is added to aluminum alloys, it strengthens the structure and improves the grain size of the aluminum. The 0.2 wt.% Sc amount used in aluminum alloy provides excellent properties in terms of grain refining without heat treatment. Other effects of Sc on Al alloys are: (1) Enhancing resistance to recrystallization by improving thermal stability [10,33,34], (2) Improving the corrosion resistance of Al alloys such as pit initiation [35] and addition of Zr shows improvement on the “EXFO”, exfoliation corrosion resistance [36] (3) Due to anti-recrystallization effect of Sc in Al it enhances super-

plasticity of the alloy [37-39]. (4) Enhancing strength [5,10]. (5) Improving resistance to hot cracking [40.41].

2.4. Mechanical Properties

Mechanical property is the form of behavior of materials when exposed to mechanical stresses. Mechanical properties are mainly related to the bond strengths between atoms; However, the microstructure of the material also has a great effect. Mechanical properties can be improved significantly by making changes in the grain structure. When the mechanical properties of the material are mentioned, the following properties should be considered, tensile and compression, hardness, impact, fracture, fatigue, and creep. It is essential to understand the mechanical behavior of materials for mechanical design and manufacturing [42].

2.4.1. Tensile Test

The tensile test is the most important and widely used destructive material inspection method used to determine the strength of metallic materials under static loads. In this method, the resistance of samples with rectangular cross-section, circular cross-section type and different geometric shapes against tensile stress as a result of subjecting to tensile force is investigated [42,43]. The main purpose of the tensile test is to measure the durability of the material. Material strength can be measured by the force that must be loaded in order for the material to undergo physical deformation or by the highest stress the material can withstand [44].

The samples are connected to the device in a way that they are located between the jaws, one is fixed, and the other is movable, and uniaxial load is applied. The applied tensile force is continuously increased at a constant speed and temperature until the sample is fractured. The tensile force applied to the sample during the test is recorded along with the elongation value of the sample and time. As a result of this information, the Load-Elongation ($F - \Delta L$) Curve and the Stress-Strain ($\sigma - \varepsilon$) curve of the material are obtained [42,43].

In summary, tensile test steps can be listed as follows.

- Selection of the material to be tested for tensile testing.
- Preparation of the sample in accordance with the standards
- Adjusting the tensile test device settings
- Tensile testing in accordance with test procedures
- Recording and analyzing tensile test data
- Reporting of tensile test results.

2.4.1.2. Tensile Test Parameters

The interpretation of the test parameters and graph obtained after the tensile test can be explained as follows (Figure 2.4) [42-44]

Stress: The load acting on the unit area is indicated by the symbol Stress (σ) and is calculated by the following formula.

$$\sigma = \frac{F}{A_0} \tag{2.1}$$

where, F is Load applied to the sample and A_0 is Cross-sectional area of the sample.

Strain: Strain is the elongation that corresponds to the unit length. It is calculated by the formula below.

$$\%\varepsilon = \frac{li - l0}{l_0} = \frac{\Delta l}{l_0} e = \frac{\Delta l}{l_0} \tag{2.2}$$

% ε: percent strain change, Δl: elongation amount of the sample, l_i: length of the sample at the time of selection, l_0: initial length of the sample.

Elastic modulus: Elastic modulus is the ratio of stress to elongation in proportional strength.

$$E = \frac{\sigma}{\varepsilon} \tag{2.3}$$

Elasticity Limit: It is the boundary point where the plastic deformation of a material begins. It is the point where there is the greatest stress at which the material can take its original shape by removing the load applied to the material.

Yield Strength: yield is the point where elastic deformation ends and plastic deformation begins in a material. Yield stress is the stress value at the point where plastic deformation begins. The stress value at this point is denoted by σ_A and calculated by the following equation.

$$\sigma_A = \frac{F(\varepsilon=0.2)}{Ao} \tag{2.4}$$

Resilience: Resilience is the return of the energy absorbed by a material in the elastic strain zone when the applied load is removed. It is the area under the elastic region only in the stress-strain curve.

$$Ur = \frac{\sigma a^2}{2E} \tag{2.5}$$

Toughness: It is the property of a material to absorb energy during plastic deformation. It gives the toughness of the material under the stress-strain curve.

$$Ut = \int_0^{\varepsilon k} \sigma_m \, d\varepsilon \tag{2.6}$$

Tensile Strength: It is defined as the maximum amount of load a material can carry without breaking or rupturing. It is one of the most used tensile test results due to its wide use in quality control and material standard conformities. By knowing the tensile strength, other mechanical properties such as fatigue and hardness can be predicted with the help of empirical formulas. The tensile strength, whose unit is N / mm2, is calculated by the formula below.

$$Rm = \frac{Fmax}{A_0} \tag{2.7}$$

Fmax: maximum force applied to the material, A_0: cross-sectional area of the sample.

Percent Elongation: It is a percentage expression of the ratio of the amount of elongation in the sample to the initial length of the sample and provides information about the ductility of the material. Percentage elongation increases as ductility increases, meaning that materials tend to deform more. Percent elongation after rupture is calculated with the help of the equation below.

$$\%\text{Elongation} = \frac{\Delta l}{l0} x100 = \frac{lk - l0}{l0} x100 \tag{2.8}$$

L_k: gauge length after rupture L_0: initial gauge length.

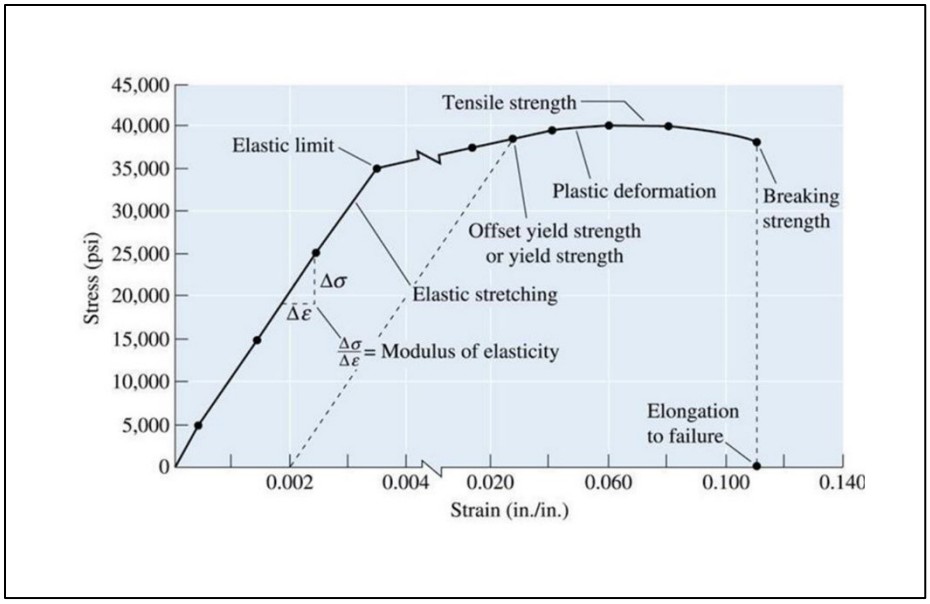

Figure 2.4. The stress-strain curve for an aluminum alloy [45]

2.4.2. Brinell Hardness

In this test (Figure 2.5), it involves applying a constant load to the surface of a solid body for a certain period (10-30 seconds), generally in the range of 500-3000 N, using a 1-10 mm diameter [46] tungsten carbide or hardened steel ball. The formula of HB number is as below:

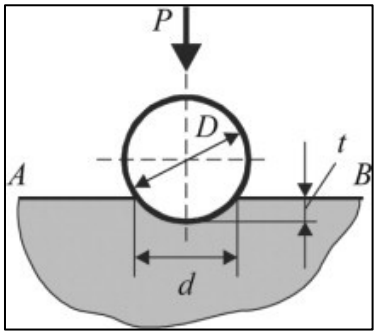

Figure 2.5. Schematic of the Brinell hardness test [47]

$$HB = \frac{P}{\pi D[D-(D^2-d^2)^{1/2}]} \quad (2.9)$$

Where:

- Ball diameter represented as D in mm,
- d represented the diameter of the recovered circular recess (mm),
- P is the applied load in kg [48].

2.5. Motivation of Study

With the developing technology, the reserves in the world are rapidly depleting. One of the examples that can be given in this field is wheel alloy. Scientists have started to search for alternative materials in this area. For this purpose, a lot of research has been done and continues to be done.

Wheels are movable equipment that works for a long time under dynamic load. For this reason, it is referred to as safety equipment. The wheels must be of high strength due to the conditions of use. In this, the grains in the structure and the spaces between them should be small.

Wheels are moving equipment that works for a long time under dynamic load. That is why it is called safety equipment. Wheels must be of high strength due to the conditions of use. In addition, it is desirable that it has a light structure. In this, the grains in the structure and the spaces between them should be small. Problems may arise due to the wheel chosen against the vehicle's weight, traction and basic characteristics. The fuel consumption of the car may increase, and the traction power may weaken due to the wheel chosen differently from the original. For this reason, the selection of wheels should not be taken lightly.

In this thesis, the search for an alternative to the additives of the A356 alloy used in wheel alloys has been discussed and the usability of the Sc element as an additive has been examined. Here, the properties of the Sc addition in the A356 alloy and whether it will exhibit a modifier or grain refiner feature in the alloy are discussed and observed in detail.

In the light of these problems, it was decided to study the addition of Sc with A356 alloy.

CHAPTER 3

EXPERIMENTAL DETAILS

In this section, studies on grain refinement, modification and heat treatment stages, which are important parameters determining the final mechanical properties of the Al – Si – Mg casting alloy system, are explained. These studies were carried out using various foundry practices, statistical methods, experimental designs, parameters, numerical values, and quantities were determined and examined in the light of professional experience. In the experimental studies carried out for the thesis study, the effect of grain refinement, modification and heat treatment on the mechanical values of the material was tried to be examined individually. T6 method was used for heat treatment. T6 heat treatment method is applied to wheel alloys due to the structure, alloy and usage conditions.

The study consists of raw material input, liquid metal preparation, degassing processes and metal mold casting stages.

3.1. Raw Material

The raw materials used in the experiments; Ready-made alloy 100% original A356.0 ingots supplied from Norwegian Aluminum manufacturer HYDRO were used.

3.2. Liquid Metal Preparation

For the production of liquid metal, a German origin, reverber type Striko tilting furnace with a capacity of 2.5 tons / hour was used. The melting temperature for the ingots is 750 ± 30 °C, and 500 kilograms of liquid metal was transferred to the FOSECO Insural 140 model transfer crucible at 770 °C.

After the liquid metal was taken into the transfer crucible, the ladle was transferred to the Rotorject model rotor degassing device made by WBB Minerals Company for degassing. In the degassing device, degassing was performed by adding 400 gr HMC – 37 flux (slag maker) (for more detail please check section 3.2.3) powder with 99.95% pure Nitrogen gas (N2) at 1 bar pressure for 4 minutes. After the process, gaseousness and chemical analysis samples were taken from the liquid metal, which fell to a temperature of approximately 745 °C, and the gaseousness was measured with the IDECO brand Thermal Analysis and Gaseousness Measurement device and chemical analysis was performed with the ARL Metals Analyzer Spectrometer. The liquid metal at 745 °C, which was approved after the analysis reports, was taken to the induction holding furnace with a capacity of 700 kg.

3.2.1. Striko Reverberatory Furnace

In this furnace with a melting rate of 2.5 tons/hour, the burners working with natural gas are positioned on the bath and the necessary heat is provided by radiation and convection resulting from combustion. The hot combustion gases released in the furnace pass through a chimney opening to the preheating zone and provide preheating to the alloy ingots loaded to be melted, making the melting process fast and economical. The furnace is a tiltable type, and the liquid metal is discharged into the transfer ladle by tilting the furnace through the hydraulic system and thus the liquid metal flows due to the slope.

3.2.2. Degassing Process

Degassing was carried out in a Rotorject model degassing device of WBB Minerals (Table 3.1). The device has been specially designed according to the flux injection process; Flux powder is injected into the liquid metal together with nitrogen gas through a rotor cylinder made of silicon carbide, which rotates at 300 rpm. Schematic Illustration of rotorject degassing device can be indicate on Figure 3.1

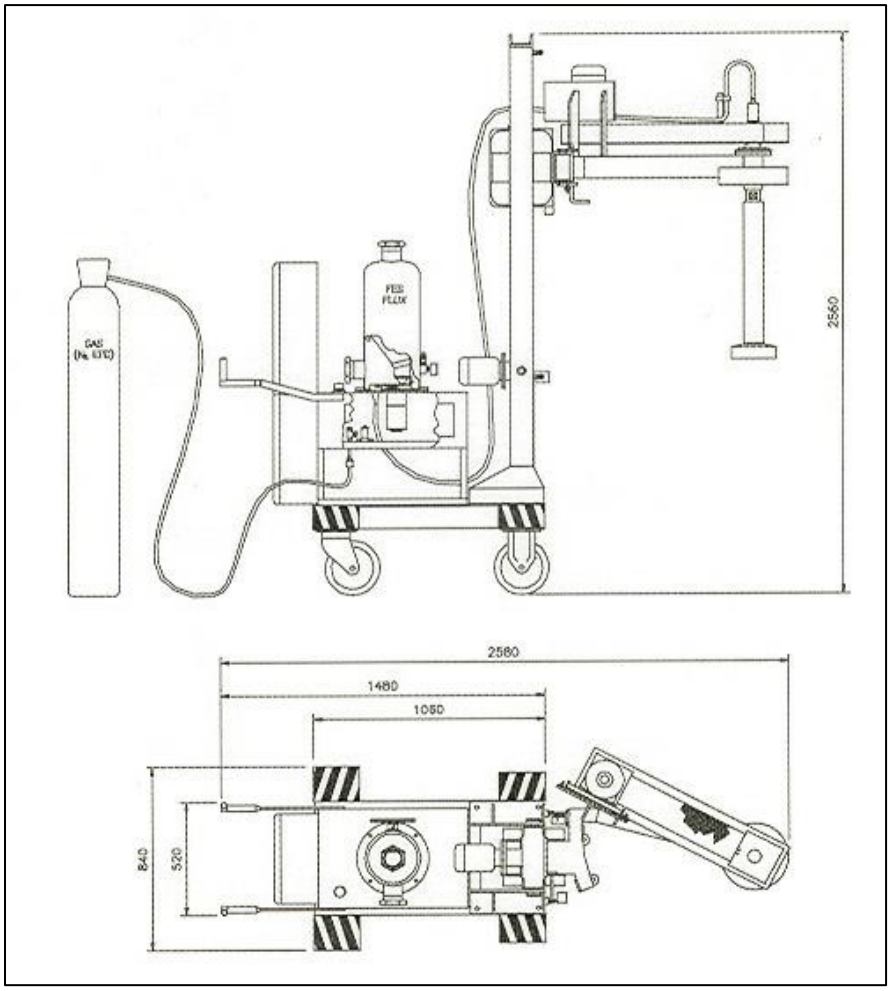

Figure 3.1. Schematic Illustration of Rotorject Degassing Device [49]

Table 3.1. Technical Data of WBB Minerals Made Rotorject Degassing Device [49]

WBB Minerals Rotorject Technical Data	
Voltage	240 / 110 V
power requirement	13 A
Frequency	50 Hz
Optional Frequency	60 Hz
Supply Voltage External Control Voltage	110 V
Control System	Automatic
Nitrogen Gas Operation	Automatic
Nitrogen Gas Supply Pressure	2 - 4 Bar (Max.)
Nitrogen Gas Working Pressure	0,3 - 1,5 Bar
Nitrogen Gas Output Pressure	0,3 - 1,5 Bar
Nitrogen Gas Supply Control	Level Control with Alarm
Nitrogen Gas Feed Time (During Process)	0 - 30 Minutes (Timer Control)
Nitrogen Gas Feed Time (Before Process)	0 - 215 Minute
Nitrogen Gas Injection Rate	Changeable
Flux Feed Rate	0 - 250 gr / min
Rotor Speed	0 - 600 rpm

3.2.3. HMC 37

HMC 37 is a white powder flux used in aluminum alloys, it is a cleaning and degassing flux that can be used with all aluminum alloys rather than other alloys that are not intolerant to sodium. HMC 37 has been specially developed for the Flux Injection Process using nitrogen as the carrier gas. This process ensures optimum contact of liquid metal and flux particles. In this way, while the flux is used very efficiently, metal cleaning is provided well.

The HMC 37 has a wide range of uses, from small crucibles to large reverberatory melting furnaces. Due to the powder structure of the flux, it has the feature of free flowing and dispersion in liquid metal. Flux injected into the liquid metal ensures the separation of oxides and impurities in the metal and the removal of trapped gases.

As a consequence of the reactions occurred during the contact of liquid metal and flux, a dry slag layer is formed and suspended on the liquid metal surface. In addition, with this flux, the slag adhering to the furnace walls can be easily dissolved, thereby facilitating the cleaning work and simplifying the repair processes.

The method of use is basically based on the following principles:

- The amount of flux to be injected should generally be 0.2 % of the total liquid metal weight. However, this amount can be increased according to the degree of contamination in the liquid metal.
- The addition of flux should be done with a Flux Feeder or Rotorject while the liquid metal is in the temperature range of 640 – 720 °C.
- After the application, the slag layer formed on the surface is peeled off and separated from the metal.

3.4. Sample-Casting

3.4.1. Mold Preparation

After the liquid metal and mold preparation processes, the casting phase was started, and as can be understood from the sprue and feeding design of the sample mold, the liquid metal was poured directly into the mold with the help of a ladle according to the gravity casting method principle. For filling the mold, a steel ladle (ST 37 standard) with a liquid metal capacity of approximately 1.2 kg was used, and it was coated with DYCOTE 34 to prevent sticking similar to the mold.

Mold was preheated to 320°C. Casting processes were carried out at a liquid metal temperature of 730 ± 15 °C. The metal temperature was measured with a Heraues Electro-Nite brand hand pyrometer before each piece was cast, and the mold temperature was measured with a RAYTEK brand laser pyrometer. The mold temperature was kept in the range of 320 ± 5 °C during all sample castings. For the solidification process, no additional cooling was applied, and the part was allowed to solidify in the mold itself. Each piece whose casting was completed was cooled by giving water in a container filled with normal mains water. After the cooling process, the marked parts were transferred to the lathe workshop for processing.

3.4.2. Sample preparation

After the sprue and runners were cut, the parts whose casting was completed were prepared in pieces, the dimensions of cut section are given in Figure 3.3. Since the tests will be done repetitively, the parts in Figure 3.3 were cut in two equal parts, marked and made ready for the tensile test.

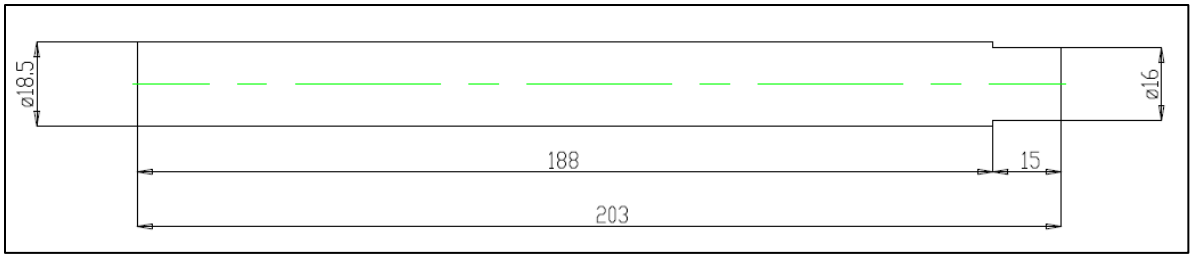

Figure 3.3. Tensile Test Bar Post Casting Dimensions (All dimensions are in mm.) [49]

The samples, whose heat treatment was completed, were machined with a lathe into a diameter of 5.64 mm and made ready for the tensile test. The technical drawing of the tensile test rod is given in Figure 3.4.

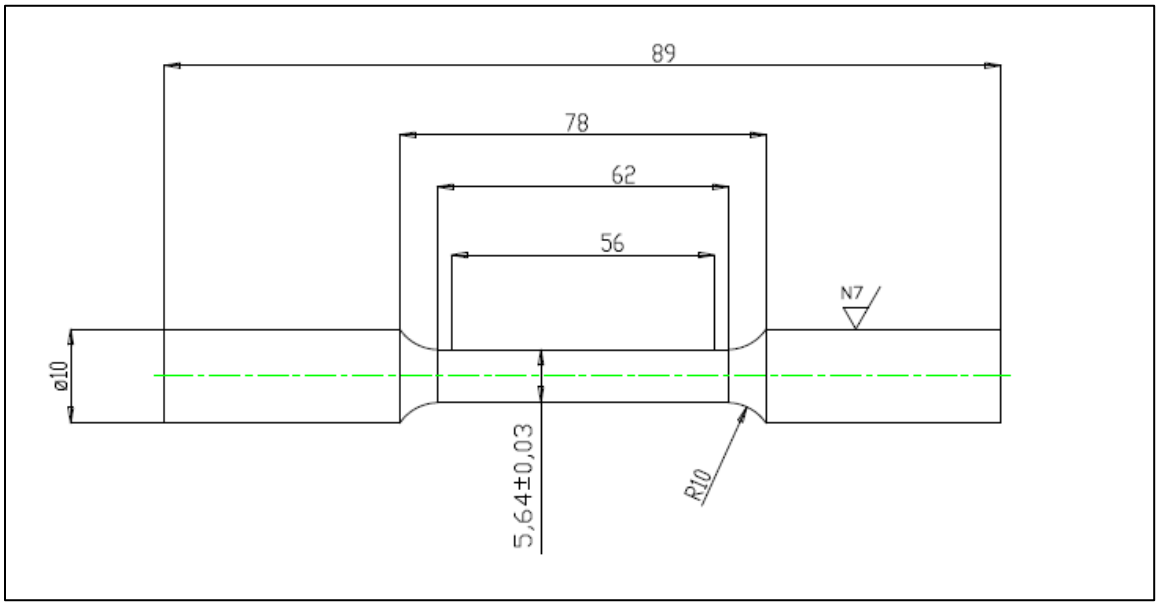

Figure 3.4. Tensile Test Sample Dimensions (All dimensions are in mm.) [49]

3.4.3. Casting

The casting process was carried out using a gravity die. In the first stage, the molds were subjected to the poteage process, and then they were preheated by heating up to a temperature of approximately 320 (± 5) ° C. A total of 4 ladle were used in the casting part of the experiment. The casting temperature was determined to be 730 (± 5) ° C. Ladles are 4 kilograms and the first ladle is A356 alloy, which is the reference alloy. The second ladle contains 0.2 wt.% Sc-A356 alloy, the third ladle contains 0.4 wt.% Sc A356 alloy and the fourth ladle contains 0.6 wt.% Sc. Casting was done twice to prevent deflections/offset that may occur in the tests. (Figure 3.5) 10 samples were obtained from each group. In the experiment, 1.6 g, 2.4 g and 8 g Sc were used for 4 kg of A356 alloy. After casting processes, samples were first cooled in open air and then subjected to T6 heat treatment. In the heat treatment, the processes of taking into solution, quenching and holding at 550 degrees were realized. After the heat treatment, the samples were subjected to tensile testing. (Figure 3.4)

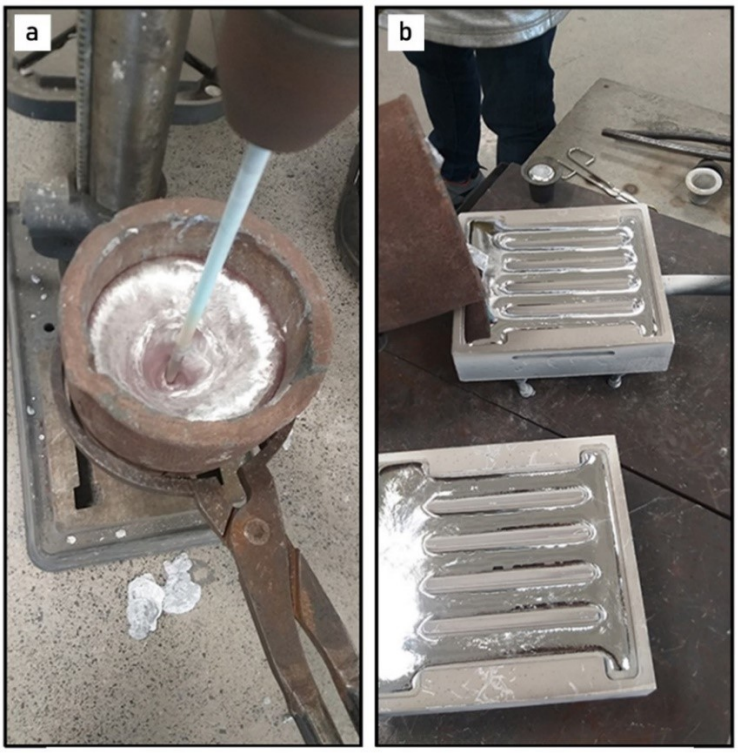

Figure 3.5. (a) Casting of Sc-A356 Alloy, (b) Casting alloys into molds for tensile testing.

3.4.4. Tensile Test

Tensile tests of all samples were carried out in accordance with EN ISO 10002-1 Tensile Test Standard. The material testing device is defined as an above ground tensile testing device with a maximum test load capacity of 100 kN in the technical and commercial literature. The device is specially designed for tensile testing and is suitable for testing ferrous and non-ferrous metals, hard and reinforced plastics, wood, and similar materials [50].

Tensile bar samples for the tensile test were prepared as 10 samples for each test group. The prepared samples were measured with the "Zwick Z100/SN3A" model tensile tester. The amount of elongation from the tensile test was measured with an extensometer. The results were evaluated by taking the average of the tests performed for each group.

3.2. Characterization Techniques

3.2.1. Optical Microscopy

One of the most used imaging tools is the optical microscope used in many fields [51]. It is also referred as the light microscope. This microscope uses system of lenses to magnify images of small samples by using visible light [52,53]. Within the scope of this thesis, the samples were examined with a NIKON-2000 optical microscope (4X,10X,20X and 40X optical lens size).

3.2.2. Sample Preparation

500, 1000, 2000 grit size grinding papers were used in the metallographic sample preparation and then the polishing stage with 1μm etched diamond paste was applied. The samples were etched with 3% HCl acid. In order to obtain macrostructure images, the samples were prepared by going through the grinding, polishing and etching stages as stated above. Macrostructure samples were etched using FeCl acid. Sample preparation stages are given in table 3.2. Macrostructure samples are made to measure grain sizes and also to have a general idea about

grain structures. The samples were examined under a microscope and grain size measurements were made.

Table 3.2. Sample Preparation Stages

Parameters / Stages	Surface	Etching	Liquid	Rotate (rpm)
Rough grinding		500	Water	350
	Grinding	SiC		
Medium grinding		1000	Water	300
	Grinding	SiC		
Fine grinding		2000	Water	300
	Grinding	SiC		
Final Polishing		1 µm	Diamond water	270
	Broadcloth	Diamond paste		

3.2.3. SEM- Scanning electron microscopy

SEM is used to study the microstructure and morphology of materials (Figure 3.6) [54]. An electron probe Scans the surface of the material as a result of which electrons interact with the material. Secondary electrons emanate from the surface of the sample and then register. The high differences in the sample give contrast in the image. While a topographic image is taken from the surface in SE (secondary electron), contrast difference of the elements occurs in BSE (Back Scattered electron). In other words, heavy elements (higher atomic number) appear brighter because they reflect more, while lighter ones (lower atomic number) appear darker [55]. In this thesis, FEI QUANTA 250 FEG device was used.

Figure 3.6. SEM device used in the study

3.2.4. EDS

Energy dispersive X-ray analysis microanalysis are called EDS, EDX [56,57]. EDS is a technique which shows the analysis of elements near the surface and the amount of the sample at different positions on a map by using SEM [58]. This technique is based on the interaction of some X-ray excitation source with a sample. Each element has a unique atomic structure that allows for a unique set of peaks in the X-ray emission spectrum [56,57].

In addition, fracture surface analysis was carried out using the samples that broke off during the tensile test.

CHAPTER 4

RESULT AND DISCUSSION

4.1. Optical Microscopy Results

In microstructures, the grains are mostly needlelike. A needle-like wheel is more likely to break due to the dynamic force being created on the wheel while the wheel is moving. For this reason, it is preferred that the grain structure be spherical. It was observed that no sphericity was formed in the grain structure with the addition of Sc (Figure 4.1).

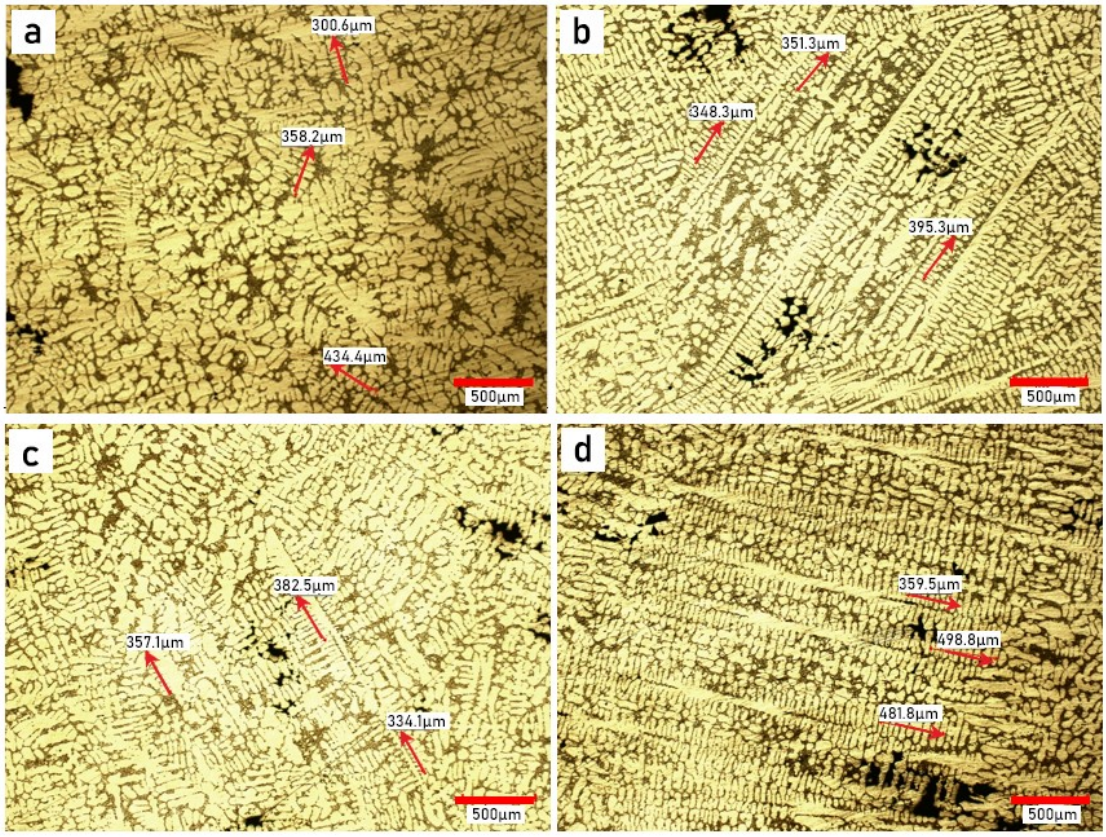

Figure 4.1. Shows (a) reference alloy (A356) with 48.50 µm dendrite arm lengths, (b) A356 - 0.2 wt.% Sc with 36.46 µm dendrite arm lengths, (c) A356 - 0.4 wt.% Sc with 35 µm dendrite arm lengths, and (d) A356 - 0.6 wt.% Sc with 44.6 µm dendrite arm lengths under optical microscopy

According to DAS (Dentritic Arm Spacing) measurements, adding 0.2 wt.% Sc to the reference alloy caused a shortening of 12µm in dendrite arm lengths. Dendrite arm lengths continued to decrease as the amount of Scandium continued to increase. After exceeding 0.4 wt.% Sc, dendrite arm lengths started to increase again. According to DAS measurements, an increase in the amount of Scandium up to 0.4% by weight decreases the dendrite arm lengths. Fracture strength and crack growth show that it is better than the reference alloy. It was observed that dendrite arm lengths increased after the Sc amount exceeded 0.4% by weight (Figure 4.2). This situation causes the mechanical properties to decrease.

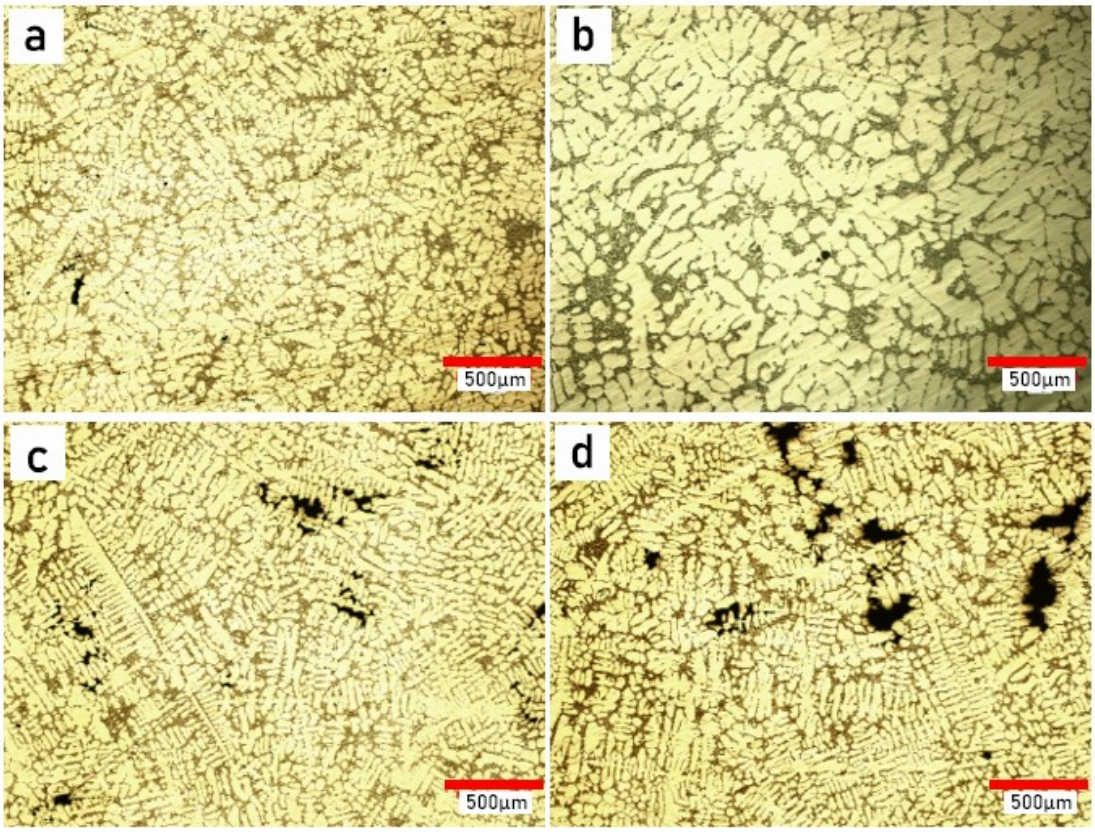

Figure 4.2. Shows (a) reference alloy (A356) with 3.89 µm porosity, (b) A356 - 0.2 wt.% Sc with 2.45 µm porosity, (c) A356 - 0.4 wt.% Sc with 3.58 µm porosity, and (d) A356 - 0.6 wt.% Sc with 4.28 µm porosity under optical microscopy

According to the porosity measurements, added Sc by 0.2 % in weight to the reference alloy caused a decrease in the porosity amount. As can be seen from Figure 4.3 it has been observed that the increase in the amount of Sc to greater than 0.2 wt.% causes an increase in the porosity ratio. Increase in the amount of porosity will decrease the mechanical strength of the material as well as cause crack formation and increase in crack propagation. It was observed that adding 0.2 wt.% Scandium by weight decreases the amount of porosity, so it is the best sample in terms of mechanical strength, crack formation and progress.

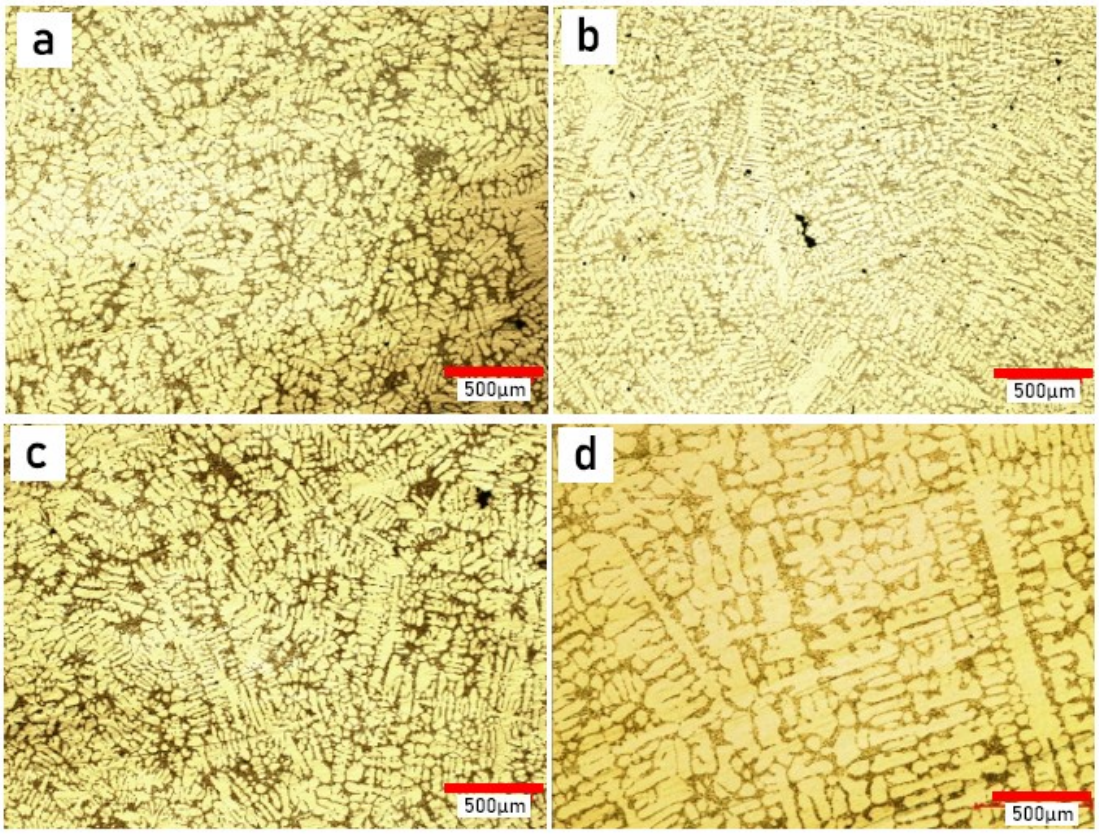

Figure 4.3. Shows (a) reference alloy (A356), (b) A356 - 0.2 wt.% Sc, (c) A356 - 0.4 wt.% Sc, and (d) A356 - 0.6 wt.% Sc under 500 µm in optical microscopy

It was determined that the addition of 0.2 % Sc by weight provided thinning in the grain structure in the microstructures (under 500 µm). Addition of 0.4% Sc resulted in reduction in dendrite arms. It has been observed that adding 0.2 % Sc by weight has a grain refining effect. As seen in the microstructures, the silicon length in the eutectic regions has been observed to decrease

greatly due to the scandium addition. The shape of the silicon was observed to change from needle to spherical shapes with the addition of scandium, thus exhibiting the well-known phenomenon of modification (Figure 4.4).

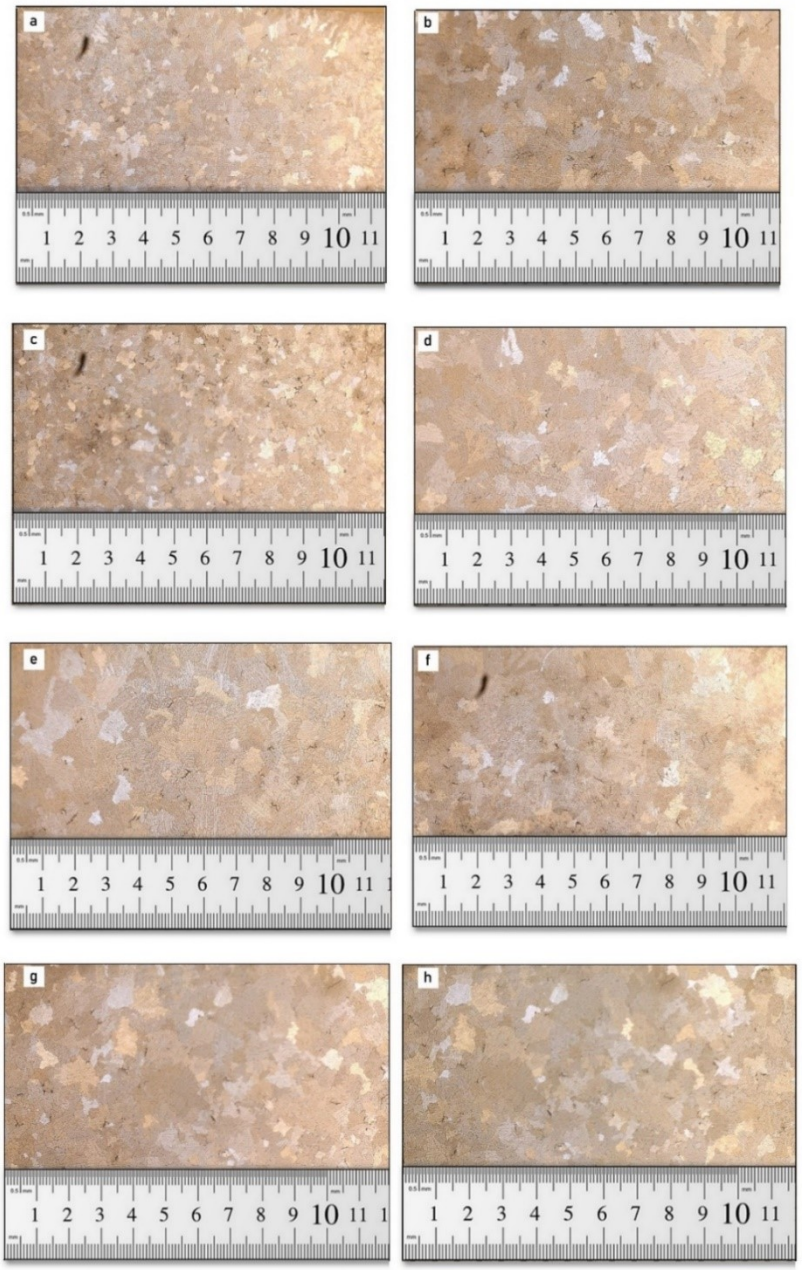

Figure 4.4. Represent sample number (a) A356-Ref1, (b)A356-Ref2, (c) A356 - 0.2 wt.% Sc-Sc3, (d) A356 - 0.2 wt.% Sc-Sc4, (e) A356 - 0.4 wt.% Sc-Sc5, (f) A356 - 0.4 wt.% Sc-Sc6, (g) A356 - 0.6 wt.% Sc-Sc7 and (h) A356 - 0.6 wt.% Sc-Sc8.

4.2. Grain Size Analysis

According to the measurements, adding Scandium did not make a visible contribution to the grain size. It was observed that the addition of 0.2 wt.% Sc caused a decrease in grain size of 38μm on average, while the increase in the amount of Scandium caused significant increases in the grain size. Figure 4.4 shows macrostructure of each sample. The general grain size average is presented in table 4.1 in order to be easy to compare.

Table 4.1 Comparison of Average Grain Size of each sample

Alloy	Average Grain Size (micrometer)	Percentage change of grain size by reference
Reference Alloy	709.8	-
0.2 wt.% Sc Content alloy	671.5	-5.70%
0.4 wt.% Sc Content alloy	774.8	8,39%
0.6 wt.% Sc Content alloy	750.1	5,38%

Due to the high dynamic load on the wheel, the wheel strength is expected to be high. One of the factors that increase the strength is the grain size. If this phenomenon is large in a structure, the strength decreases, if the grain size is small, the strength increases. Smaller grain structure increases the strength as it will reduce the space between the grains and bring the grains closer together. However, it was observed that the addition of Sc caused an increase in grain size compared to the reference alloy. Therefore, the addition of Sc did not show an increase in strength.

4.3. Tensile Test Result

The tensile test results are given in Figure 4.5 and details about the test result given in table 4.2 at below. Tensile curve for each specimen are given in Figure 4.6 up to 4.9 at below. Comparison stress value for samples are given at Figure 4.10.

In the tensile test results, it was observed that 0.2 wt.% Sc addition increased the elongation of the alloy by 3% compared to the reference alloy. It has been determined that as the Sc ratio increases, it causes decreases in mechanical strengths such as yield strength. It has been observed that 0.2 % Sc addition increases rupture strength by approximately 10 Mpa while increasing Sc percentage decreases rupture strength. When examined in terms of quality, the addition of 0.2 wt.% Sc caused an increase in alloy properties by 35 MPa, while a high increase in Sc amount decreased this value.

Table 4.2 Comparison of samples giving the average results in tensile testing

Alloy/ Specification	Average Yield Strength (MPa)	Average Tensile Strength (MPa)	Average Elongation (%)	Percentage change of Yield Strength	Percentage change of Tensile Strength	Percentage change of Elongation Percentage Rates
Reference Alloy	182	247	5.7	-	-	-
0.2 wt.% Sc Content alloy	181	257	8.1	-0.36%	3.93%	29.25%
0.4 wt.% Sc Content alloy	172	245	6.7	-5,32%	-0,78%	-14,77%
0.6 wt.% Sc Content alloy	173	237	5.5	-4,71%	-3.98%	-4,63%

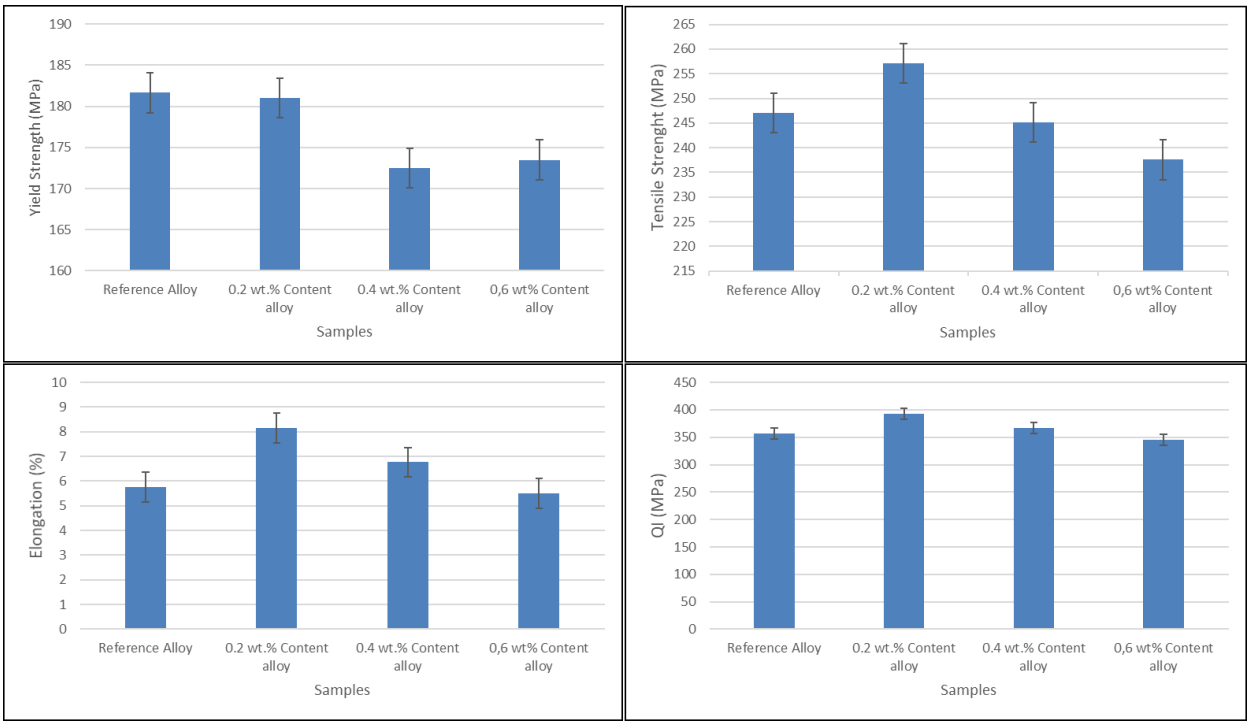

Figure 4.5. Comparison of saamples giving the average results in tensile testing

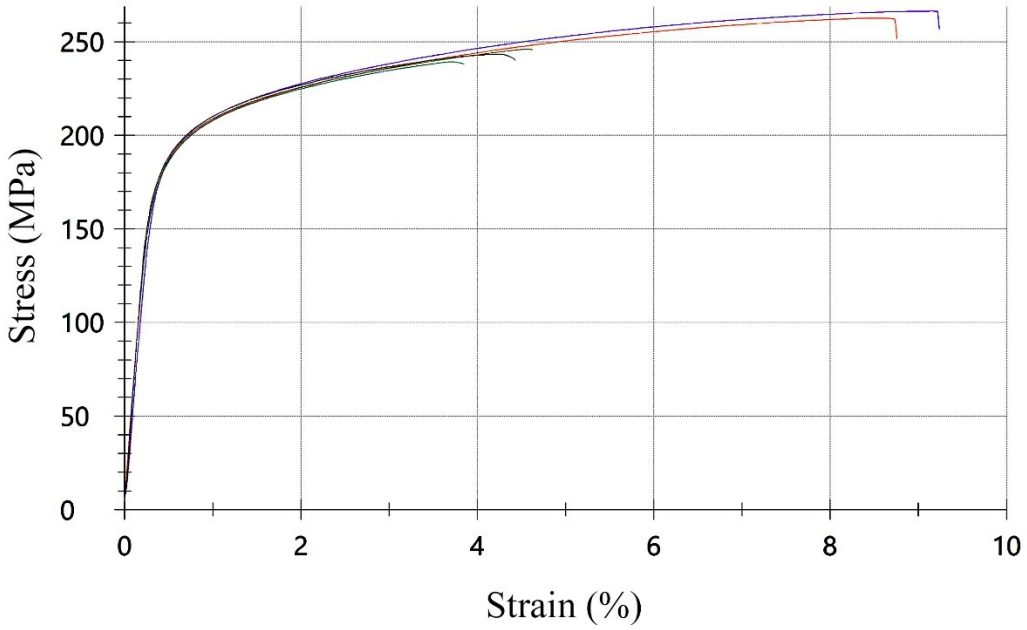

Figure 4.6. Stress-strain curves of reference samples

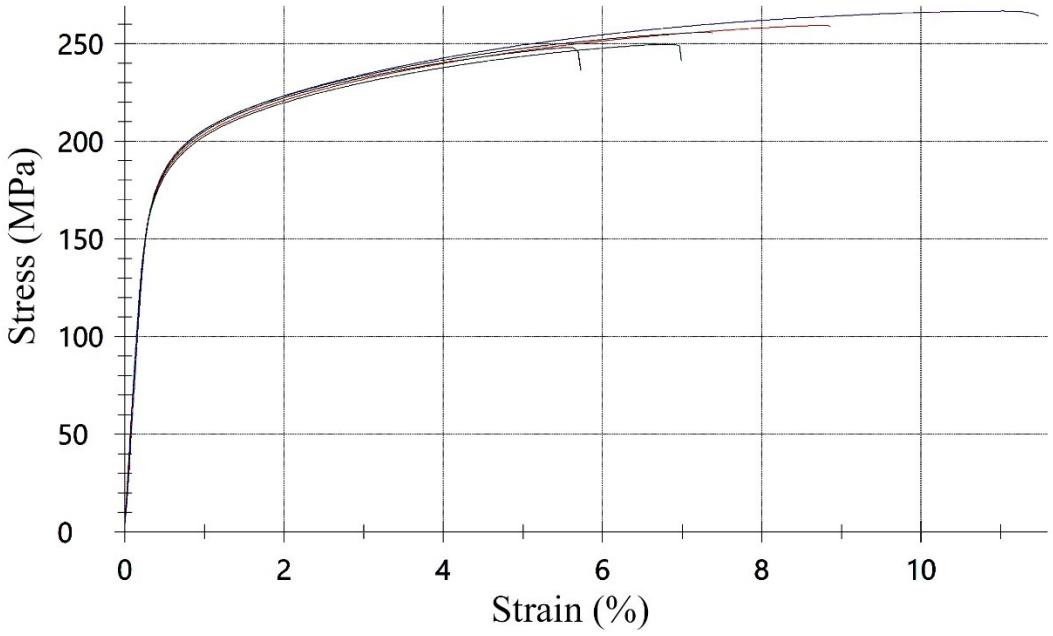

Figure 4.7. Stress-strain curves of 0.2 wt.% Sc with A356 alloy

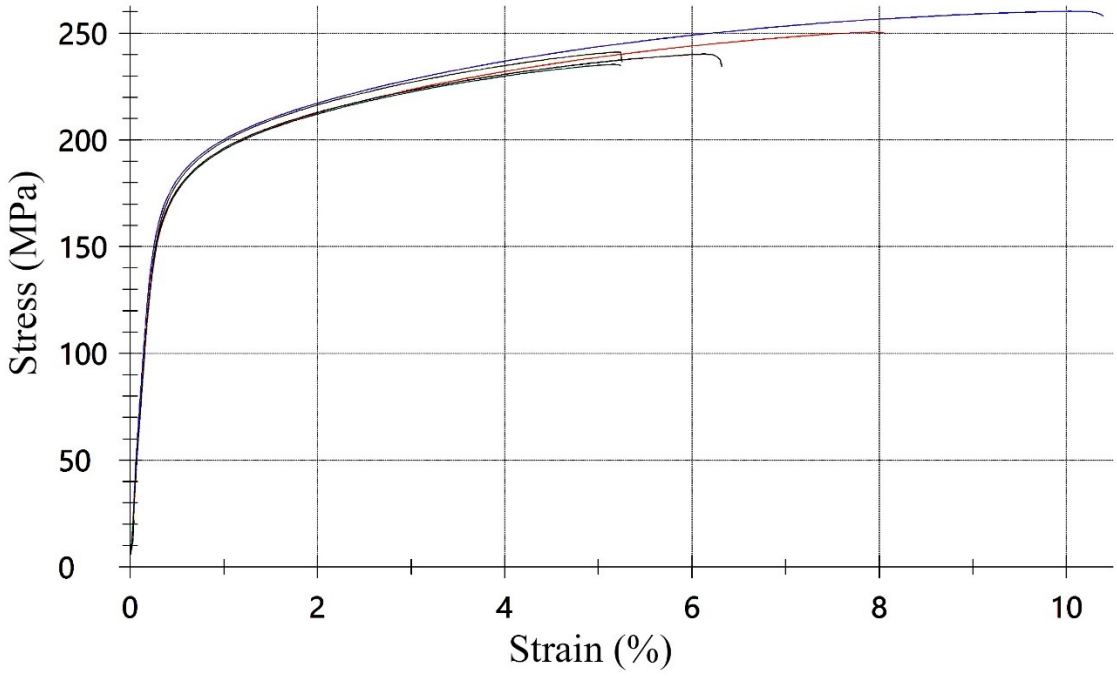

Figure 4.8 Stress-strain curves of 0.4 wt.% Sc with A356 alloy

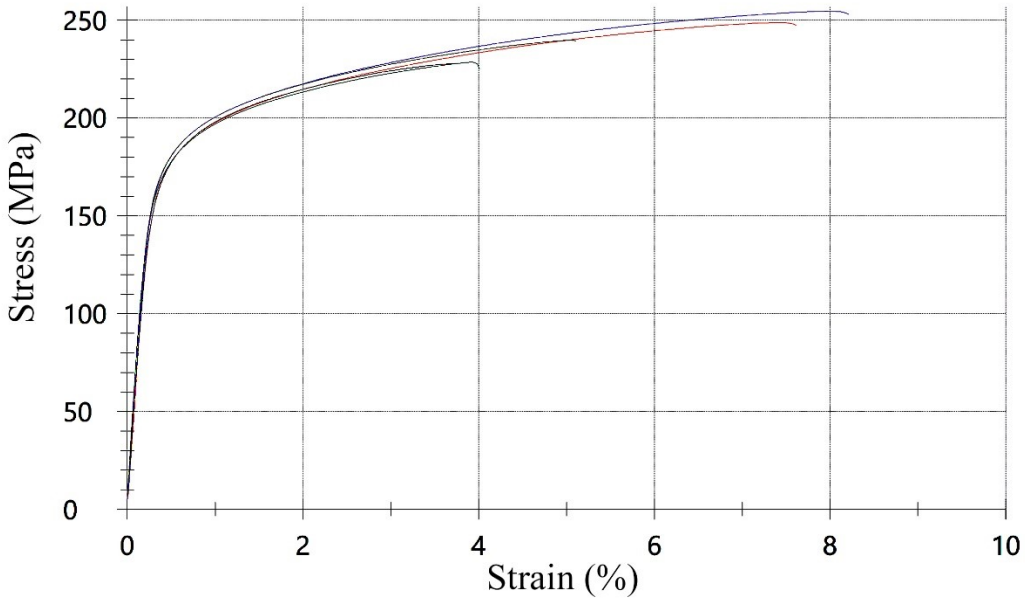

Figure 4.9. Stress-strain curves of 0.6 wt.% Sc with A356 alloy

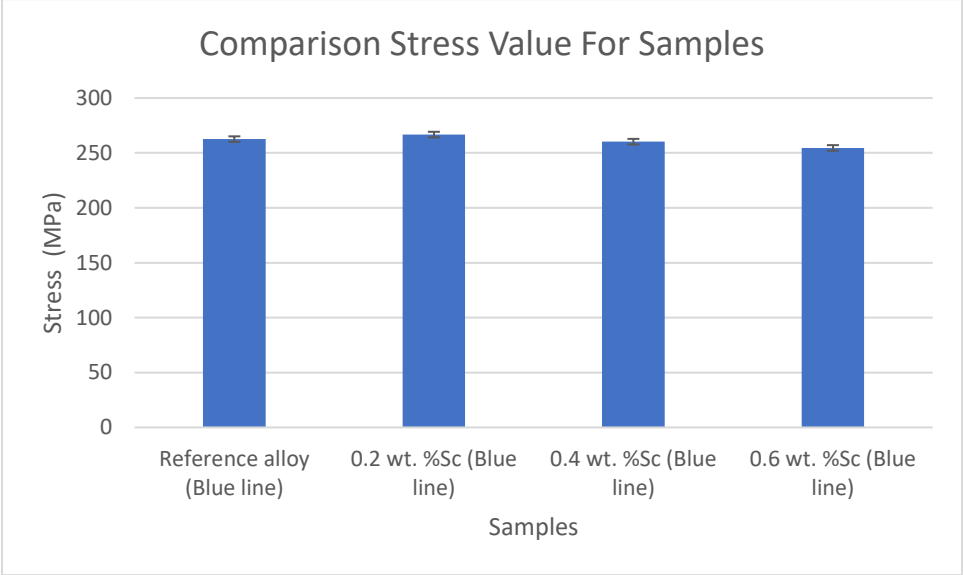

Figure 4.10 Comparison stress value for samples

4.4. Hardness Test Result

The addition of 0.2 % Scandium by weight did not show a noticeable increase on the hardness compared to the hardness value of the A356 reference alloy, while the increase in the Scandium ratio caused a decrease in the hardness values. Table which shows effect of %Sc on hardness measurements (in appendix). In here measurements were made by taking two measurements from each sample. Table 4.3 shows general hardness measurements in average and Figure 4.10 represent comparison of hardness between samples.

Table 4.3. General average of hardness measurements obtained from each sample.

	Average (HB)	Percentage change of hardness value by reference
Reference Alloy	75.77	-
0.2 wt.% Sc Content alloy	77.29	1.96%
0.4 wt.% Sc Content alloy	73.29	-3,38%
0.6 wt.% Sc Content alloy	74.39	-1,86%

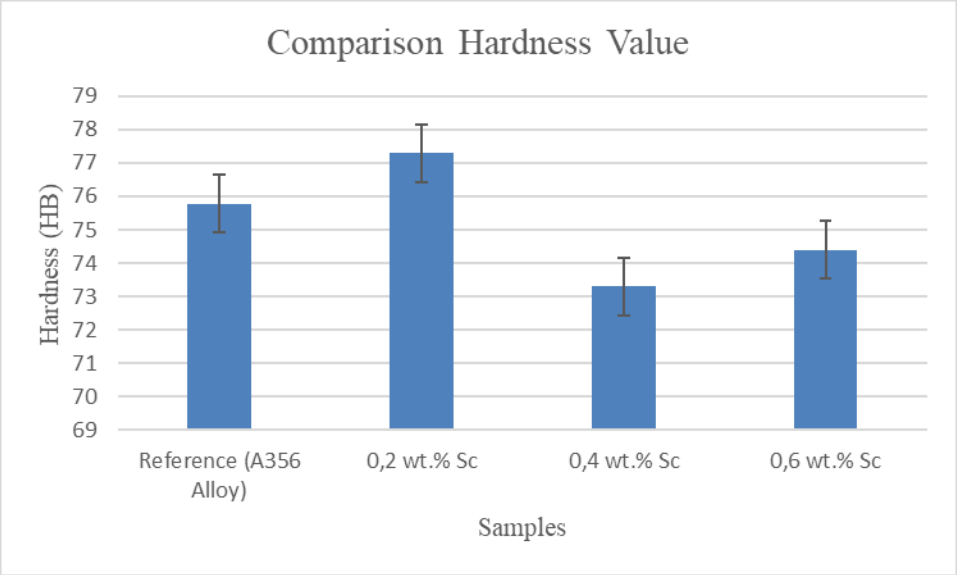

Figure 4.11. Comparison between hardness of each sample

4.5. SEM Results

SEM results are shown in Figure 4.12 and Figure 4.13. According to the SEM Micrographs, it was found that the addition of Scandium at the rate of 0.2 and 0.4 wt.% Sc caused shortening of the dendrite arms. Addition of 0.6 wt.% Sc caused a visible increase in dendrite arms. When the structures were examined, it was concluded that the amount of porosity increased in direct proportion with the increase of the amount of Sc. In addition, although it has a ductile structure in terms of fracture behavior, there are indications of brittle fracture states.

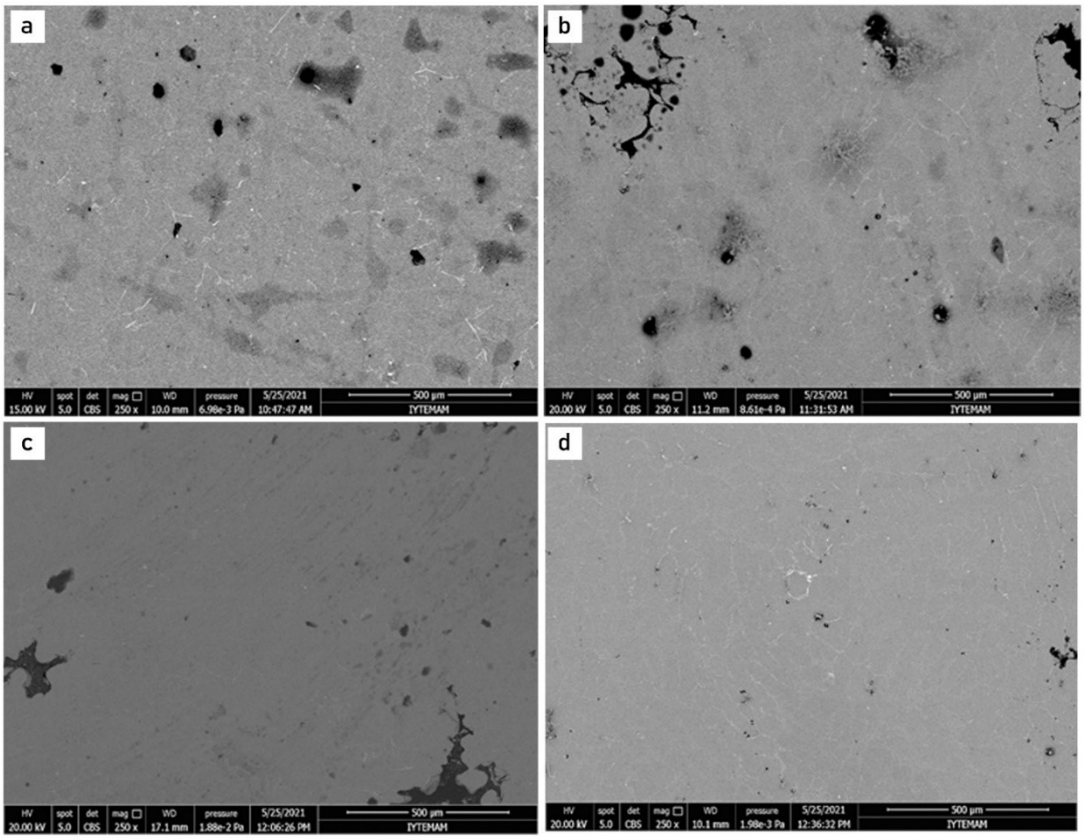

Figure 4.12. SEM Micrographs (a) A356 without Sc 250x magnification, (b) A356 with 0.2 wt.% Sc 250x magnification, (c)A356 with 0.4 wt.% Sc 250x magnification, (d)A356 with 0.6 wt.% Sc 250x magnification

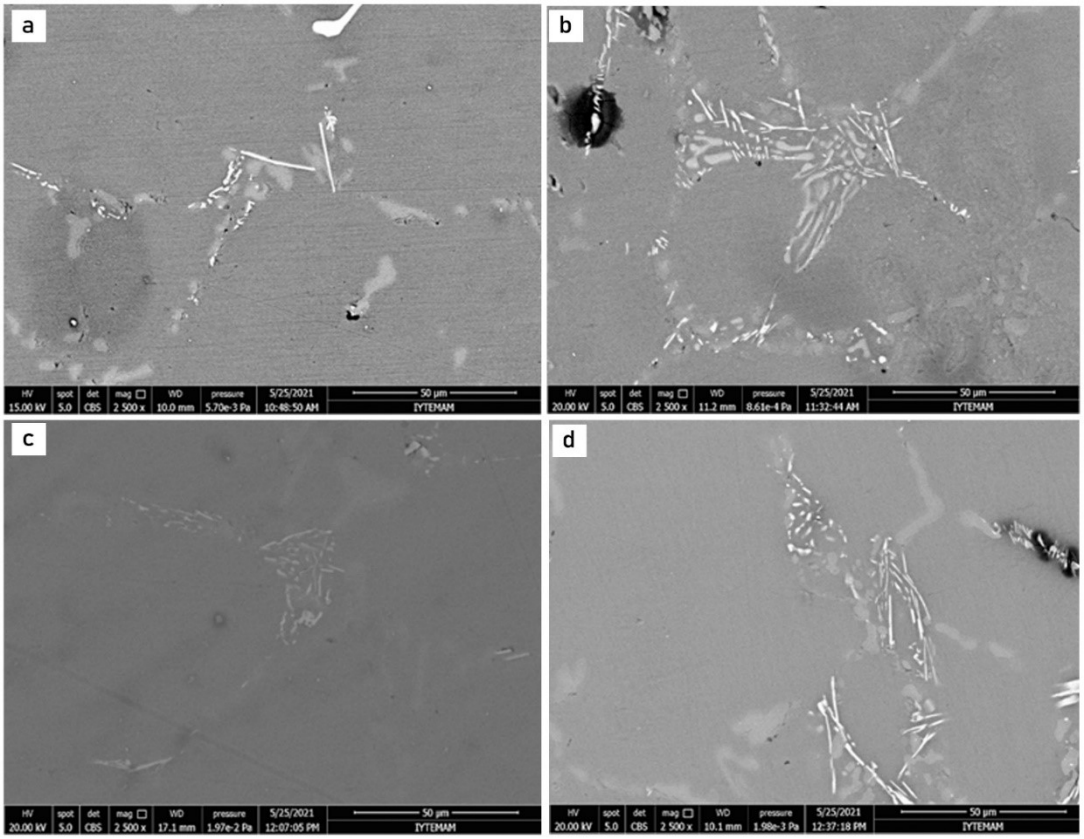

Figure 4.13. SEM Micrographs (a)A356 without Sc 500x magnification, (b) A356 with 0.2 wt.% Sc 500x magnification, (c)A356 with 0.4 wt.% Sc 500x magnification, (d)A356 with 0.6 wt.% Sc 500x magnification

It can be seen in Figure 4.14 and Figure 4.15 that the addition of scandium causes a decrease in the amount of ductility. In addition, it was observed in the obtained SEM images that the porosity ratio increased with the increase in the amount of Sc.

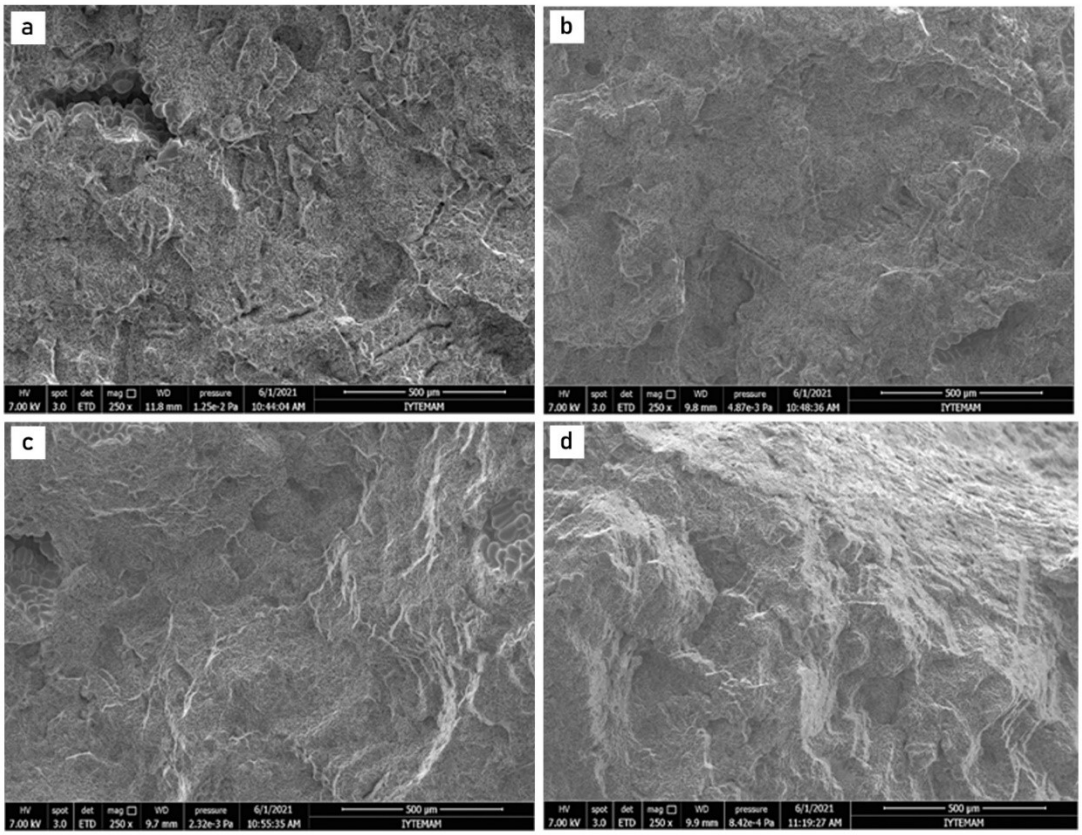

Figure 4.14 SEM micrographs (a) A356 without Sc 250x magnification, (b) A356 with 0.2 wt.% Sc 250x magnification, (c)A356 with 0.4 wt.% Sc 250x magnification, (d)A356 with 0.6 wt.% Sc 250x magnification,

In the SEM analysis, it was observed that the grain structure was needle-like. Needle-like structures reduce the strength values. For this reason, it is desirable that the grains are spherical in structures where high strength values are desired. It was observed that the addition of scandium element increased the needle-like structure in the samples examined. In addition, as the amount of Sc increased, it was observed that the dendrite arms extended. The increase in dendrite arm lengths is directly proportional to brittleness, and the strength of the structure decreases as the dendrite arm length increases. The addition of scandium did not cause an increase in the strength values, and it was found that the strength decreased due to the reasons stated.

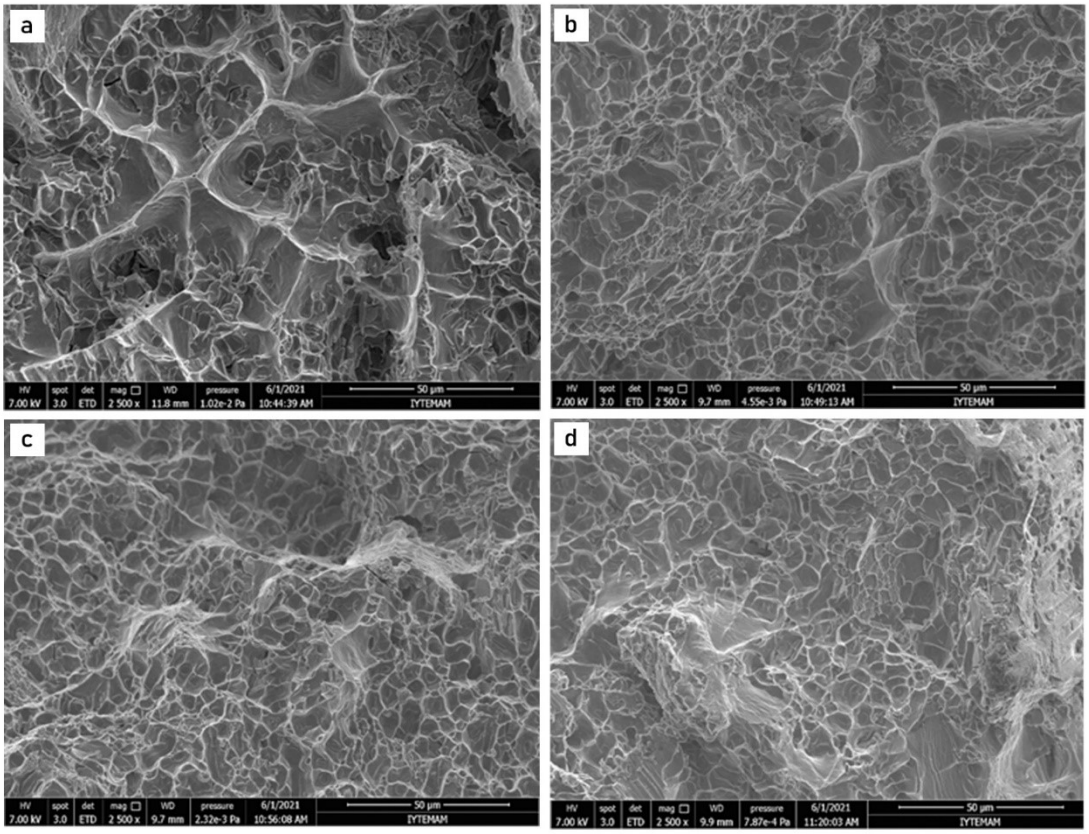

Figure 4.15. SEM micrographs (a)A356 without Sc 500x magnification, (b) A356 with 0.2 wt.% Sc 500x magnification, (c)A356 with 0.4 wt.% Sc 500x magnification, (d)A356 with 0.6 wt.% Sc 500x magnification

At the addition of 0.2 wt.% Sc, the fracture appears as ductile. Obviously, if this situation is associated with the tensile test results, it is also a proof of the increase in material toughness. However, with the increase in the amount of Sc added, this turns into the results of the reference sample. In other words, the increase in the amount worsens the mechanical properties, which is an indication of the acquisition of similar images with the reference in SEM images.

4.6. EDS Results

Spectrometer measurements could not be taken from the samples because the determined Sc amounts were below the spectrometer resolution limits.

As shown in Figure 4.16 when the Eds results were examined, Sc element was found in the star and hashtag region spectrum in the samples containing only 0.6 wt.% Sc. In the spectra taken, it was observed that the Sc structure was not homogeneously distributed. No Sc element was found in the eds analyzes of other samples. Details about star and hashtag region spectrum are given in table 4.4 and table 4.5 respectively. EDS mapping of A356 with 0.6 wt.% Sc at 2.5µm is represented in Figure 4.17.

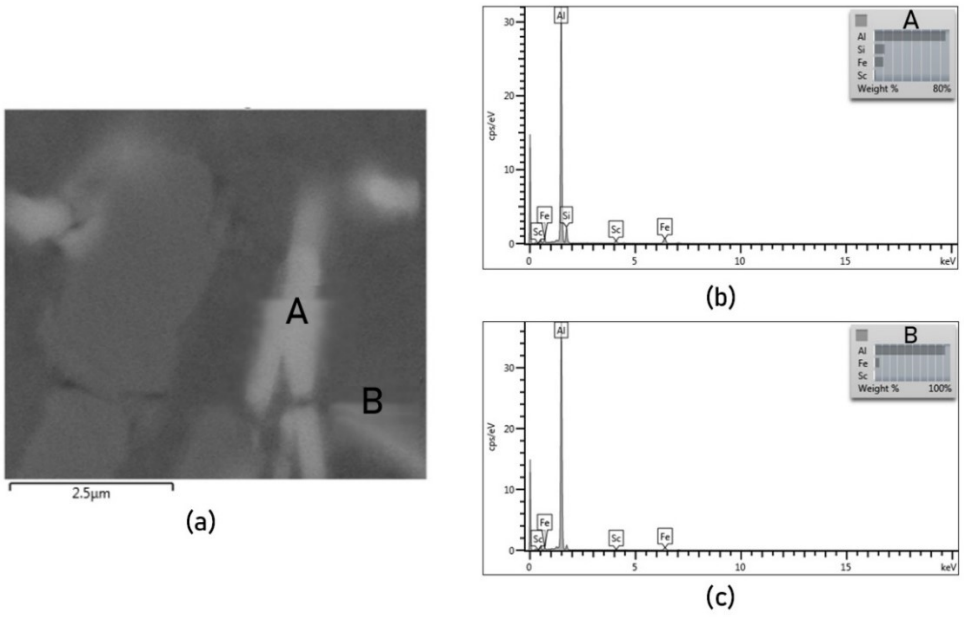

Figure 4.16. Represented spectrums received when examining EDS results as (a) EDS (Energy Dispersive Spectrometry (b) A and (c) B

Table 4.4 Area A

Element	wt.%	Atomic %
Al	75.80	81.23
Si	11.67	12.01
Sc	2.14	1.37
Fe	10.40	5.38
Total:	100.00	100.00

Table 4.5 Area B

Element	wt.%	Atomic %
Al	93.08	96.50
Sc	0.2 6	0.16
Fe	6.67	3.34
Total:	100.00	100.00

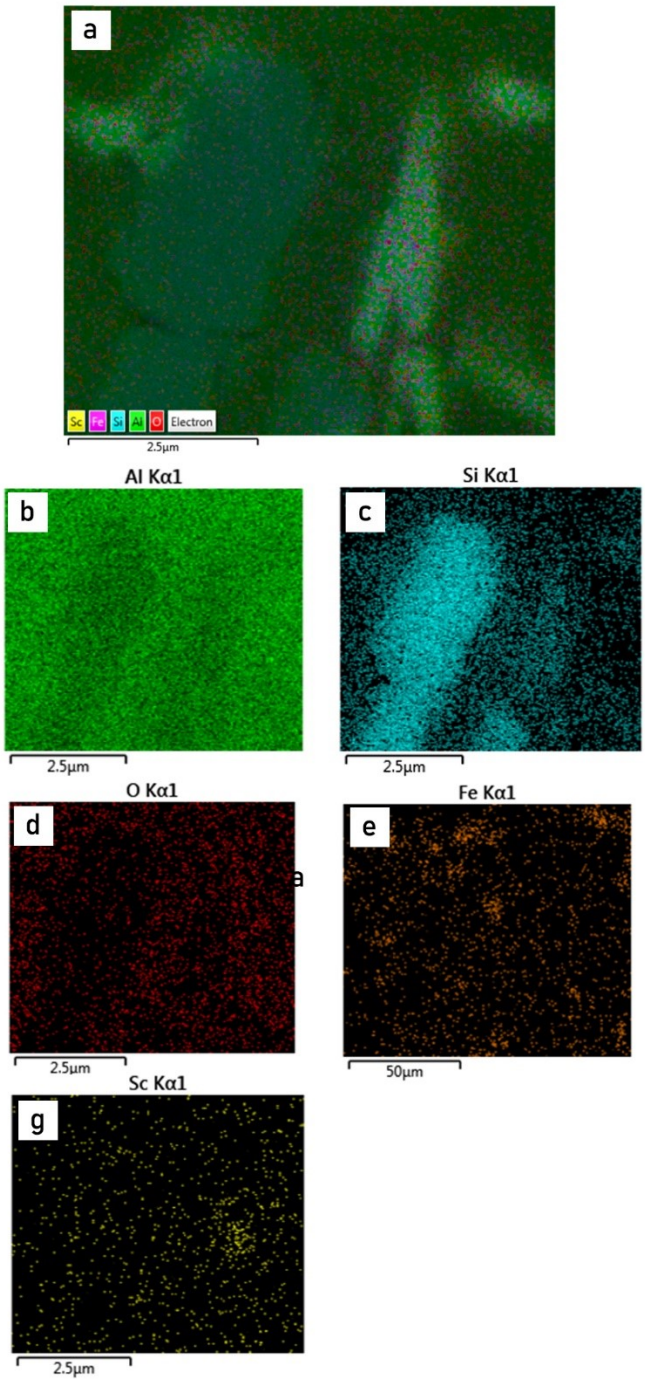

Figure 4.17. Shows EDS mapping of A356 with 0.6 wt.% Sc.

Considering the EDS results, Sc element was found in the rectangular and circle region which containing 0.4 wt.% Sc (see Figure 4.18). Table 4.6 and table 4.7 Area “A” and Area “B” region spectrum contents, respectively. In the spectra taken, it was observed that the Sc structure was not homogeneously distributed. No Sc element was found in the EDS analyzes of other samples. A356 with 0.4 wt.% Sc EDS and A356 with 0.6 wt.% Sc EDS mapping are illustrated in Figure 4.19 and Figure 4.20, respectively.

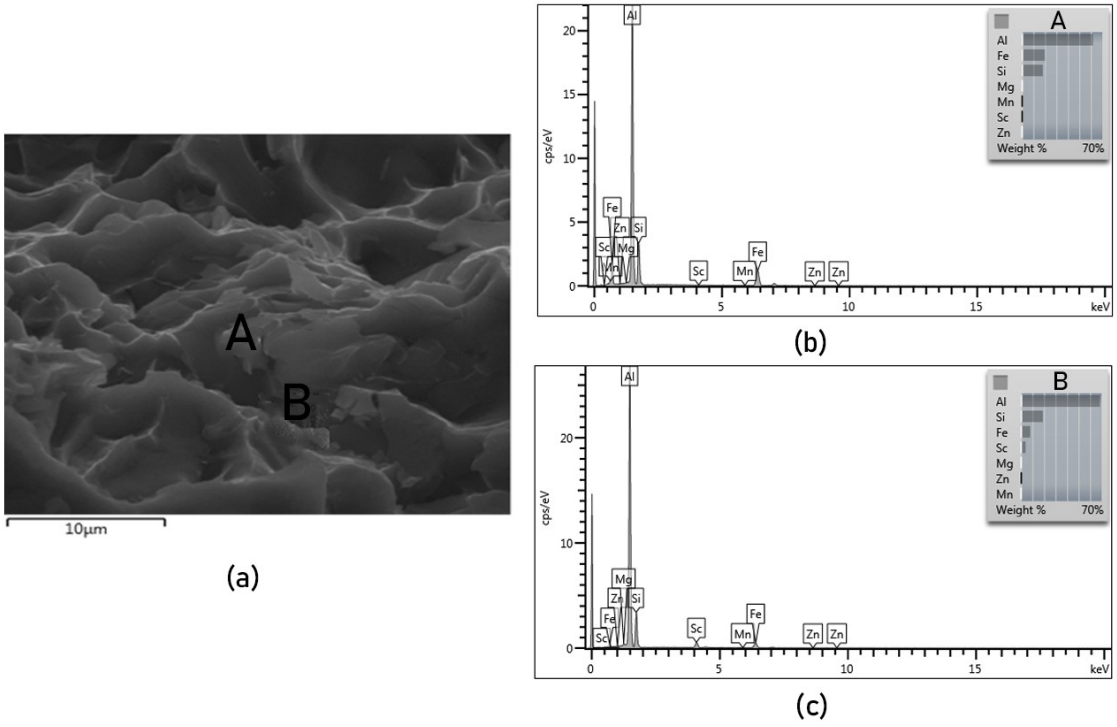

Figure 4.18. Represented spectrums received when examining EDS results as (a) EDS (b) Area A and (c) Area B

Table 4.6 Area A

Element	wt.%	Atomic %
Mg	0.14	0.18
Al	61.75	69.41
Si	18.11	19.56
Sc	0.02	0.01
Mn	0.08	0.05
Fe	19.89	10.80
Zn	0.00	0.00
Total:	100.00	100.00

Table 4.7 Area B

Element	wt.%	Atomic %
Mg	0.49	0.58
Al	68.57	73.27
Si	18.97	19.48
Sc	3.97	2.54
Mn	0.00	0.00
Fe	7.96	4.11
Zn	0.03	0.02
Total:	100.00	100.00

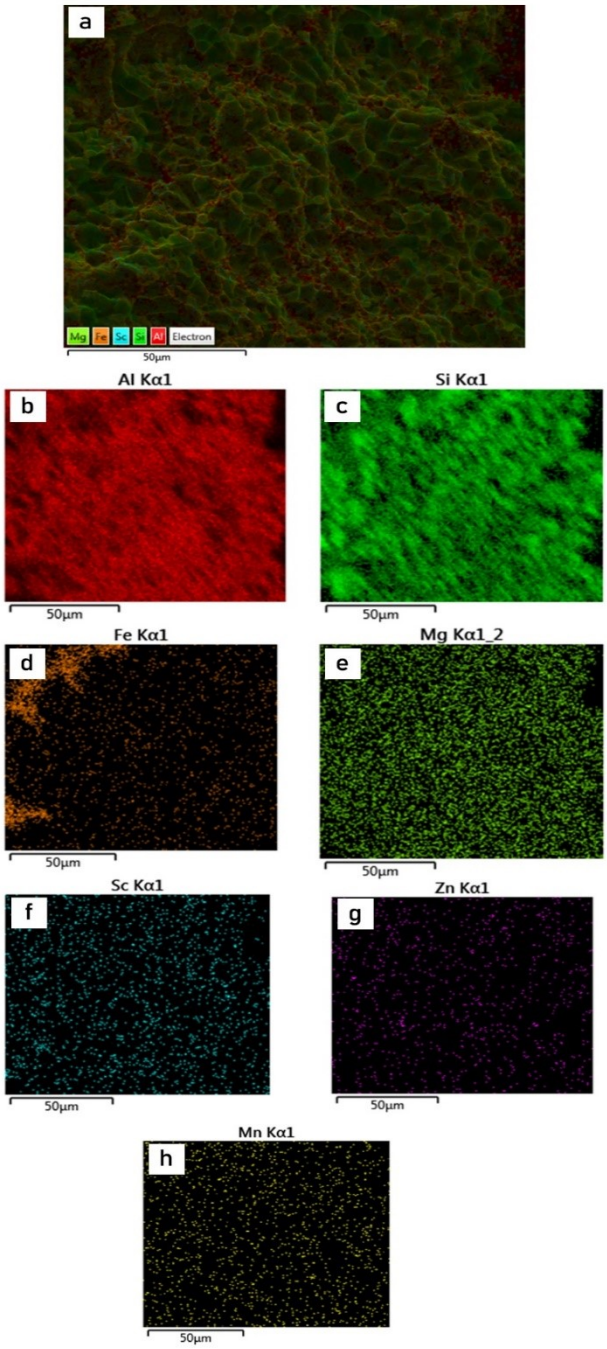

Figure 4.19. A356 with 0.4 wt.% Sc EDS mapping

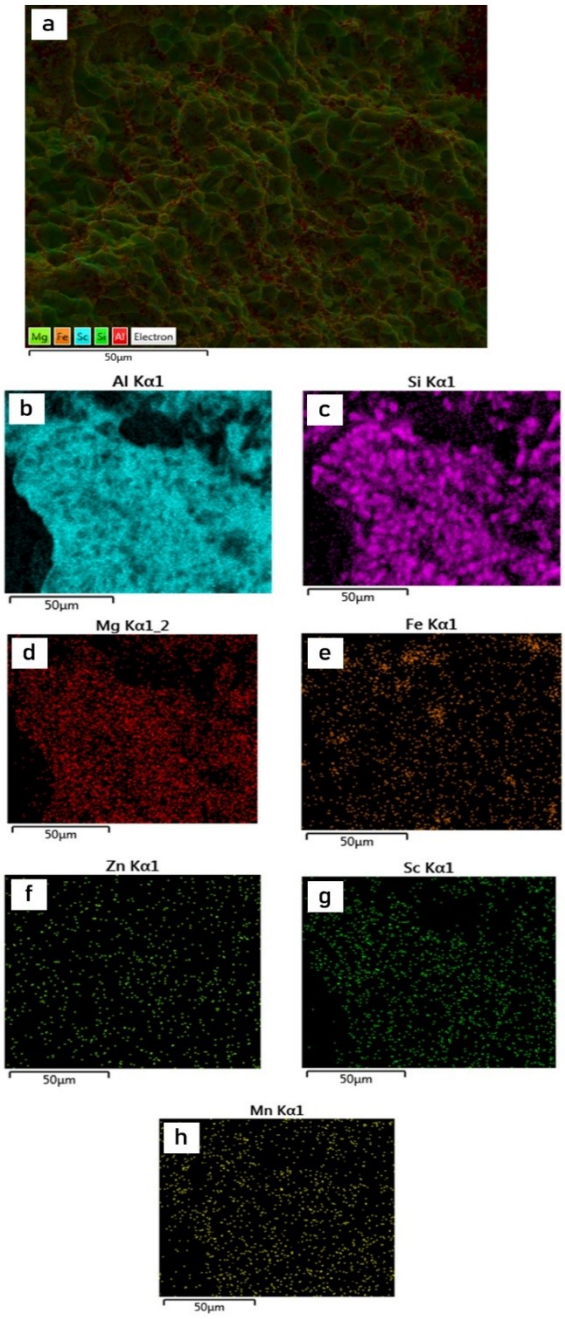

Figure 4.20. A356 with 0.6 wt.% Sc EDS mapping

EDS method was applied to determine the Sc ratios in the structure. As understood from the EDS results, Sc is not homogeneously distributed in the structure. Therefore, Sc element was not found in every spectrum taken. The homogeneity of the structure in the casting ensures the same feature to be seen in all regions on the material. In cases where the structure is not

homogeneous, the same feature cannot be seen in every region on the material. Therefore, the material is not reliable. A homogeneous structure is desired, especially in structures that are exposed to high and dynamic strength, to show the same feature from every part of the structure. Since Sc is not homogeneously dispersed in the structure, it is inappropriate for wheel alloy.

In general, it has been concluded that the addition of Sc is preferred to improve the mechanical properties of the A356 alloy. The results obtained were compared with other literature studies and it was observed that similar results were obtained. As an illustration, Zhang et al. [58] show that Al-Sc alloys showed excellent resistance to high-speed impact. In another study, cast Al-Mg-Sc containing nearly 0.16% by weight of Sc was able to improve tensile strength by ~19% and microhardness by ~30% compared to the Sc free alloy by Lathabai & Lloyd's [60]. Y.-C. Tzeng et al. [61] investigate the Sc effects on tensile properties of Al–7Si–0.6Mg. They found that the ductility of the alloy was significantly improved by addition of ~0.04 wt.% Sc, whereas increasing the Sc content up to ~0.13 wt.% gave a negligible increasing to the ductility of the alloy. Y. P. Lim et al. [62] shows that 0.2 wt.% scandium has the potential to improve tensile strength by ~27%.

They also found that the improvement of ~13% and ~149% in the Vicker's hardness and Charpy impact strength, respectively with 0.3 wt.% Sc addition to the alloy. S.L. Pramod et al. [12] investigated the wear and hardness of A356 alloy with Sc and TiB_2 added alloy. They showed with 0.4 wt.% Sc alloy and 0.4 wt.% Sc–10 wt.% TiB_2 composite hardness of the material increase up to 20% and 45% respectively. Another study done by S.L. Pramod et al. [63] in tensile test of Sc to A356 indicates that the addition of 0.4 wt.% Sc to the alloy enhance ductility, the hardness, yield strength and upper tensile strength up to 30%, 20%, 20% and 25% respectively.

When the studies carried out within the scope of the thesis are compared with the literature review, it has been observed that the addition of Sc does not cause a noticeable change in the hardness value of the alloy. According to the results obtained in the study, the most ideal addition rate is 0.2 wt.% Sc, and it has been obtained that an increase in this rate leads to a deterioration in the mechanical properties of the alloy. The results found in this study are consistent with the literature.

CHAPTER 5

CONCLUSION

The effects of A356-Sc alloy were investigated. According to mechanical testing on samples, the main gains and recommendations from this study are as follows:

- In order to reach highest UTS (ultimate tensile strength) 0.2 wt.% Sc added. The improvement in tensile strength with the addition of 0.2% by weight of Sc is 6.24% compared to the unmodified A356 alloy.
- The addition of Sc did not visibly changing the Brinell's hardness value.
- The addition of 0.2 wt.% Sc provided in an increase of 2.39% over the reference on the amount of elongation. The addition of Sc over 0.2 % caused a decrease in the amount of elongation compared to the reference.
- Addition of Sc did not show any noticeable change in yield values. However, increasing the Sc ratio tends to decrease the yield value.
- Addition of 0.2 wt.% Sc provided a 5.7% provided a reduction in grain size. If the Sc ratio increased above 0.2 wt.%, an improvement in grain size was observed compared to the reference alloy. Addition of 0.2 wt.% Sc showed grain refinement.
- The increase in the amount Sc worsens the mechanical properties, which is an indication of the acquisition of similar images with the reference in SEM images.
- Addition of 0.2 wt.% Sc improvement the ductility according to the fracture surface SEM images. If we associate this situation with the tensile test results, the material toughness increased with the addition of Sc.

REFERENCES

[1] Xu, Cong.; Ma, Chaoli.; Sun, Yufeng.; Hanada, Shuji.; Lu, Guangxi.; Guan, Shaokang. Optimizing strength and ductility of Ale7Sie0.4Mg foundry alloy: Role of Cu and Sc addition. *Journal of Alloys and Compounds*. 2018, 810, 151-944.

[2] Pramod, S.L.; Ravikirana, A.K.; Rao, Prasada.; Murty, B.S.; R. Bakshi, Srinivasa. Microstructure and mechanical properties of as-cast and T6 treated Sc modified A356-5TiB2 in-situ composite. *Materials Science & Engineering A*. 2018. https://doi.org/10.1016/j.msea.2018.10.080

[3] Dorin, T.; Ramajayam, M.; Vahid, A.; Langan, T. Aluminium Scandium Alloys. *Fundamentals of Aluminium Metallurgy*. 2018, 439–494.

https://doi:10.1016/b978-0-08-102063-0.00012-6

[4] Robert, E.; Isner, Albert C.; Johnston, lewis H. Eslinger and Alvin Sinderbrand. 75/38 Primary Examiner-L. Dewayne Rutledge Assistant Examiner-W. W. Stallard Attorneys, united states patents 3,104,252 91963 Radd.

[5] Williams, C.; The Effects of Scandium and Zirconium Additions on Aluminum Mechanical Properties, Post-Braze Grain Structure, and Extrusion. 2012.

[6] Niranjan, K.; Lakshminarayanan, P.R. Dry sliding wear behaviour of in situ Al–TiB2 composites. *Mater. Des*. 2013,47, 167–173.

[7] Suresh, S.; Moorthi, N.S.V.; Vettivel, S.C.; Selvakumar, N. Mechanical behavior and wear prediction of stir cast Al–TiB2 composites using response surface methodology, *Mater. Des*. 2014, 59, 383–396.

[8] Kumar, S.; Chakraborty, M.; Sarma, V.S.; Murty, B.S.; Tensile and wear behavior of in situ Al–7Si/TiB2 particulate composites. 2008, *Wear 265*, 134–142.

[9] Mandal, A.; Murty, B.S.; Chakraborty, M. sliding wear behavior of T6 treated A356–TiB2 in-situ composites. 2009, *Wear 266*, 865–872.

[10] Røyset, J.; Ryum, N. Scandium in Aluminum Alloys, *International Materials Review*. 2005, 19-44.

[11] Prukkanon, W.; Srisukhumbowornchai, N.; Limmaneevichitr, C. Influence of Sc modification on the fluidity of an A356 aluminum alloy, *J. Alloys Compd*. 2009, 487, 453–457.

[12] Pramod a, S.L.; Prasada Rao b, A.K.; Murty a, B.S.; Bakshi, Srinivasa R. Effect of Sc addition on the microstructure and wear properties of A356 alloy and A356–TiB2 in situ composite, *Materials and Design*. 2015, 78, 85–94.

[13] Lumley, R. (Ed.). Fundamentals of aluminum metallurgy production, processing and applications. *Cambridge: Woodhead*, 2011.

[14] Totten, G.E.; MacKenzie, D.S. (Eds). Handbook of aluminum volume 2, Alloy production and materials manufacturing, NY: Marcel Dekker. 2003.

[15] Sheasby, P.G.; Pinner, R. Introduction: Aluminium, its properties, alloys and finishes. In the surface treatment and finishing of aluminum and its alloys. Materials Park, *OH: ASM International*. 2001, 6 1-10.

[16] Eruslu, N. Alüminyum alaşımlarının dökümü ve yapı kontrolü, *SEGEM Yayınları*, İstanbul, 1984.

[17] ASM Handbook Volume 2, 'Properties and Selection: Nonferrus Alloys and Special-Purpose Materials, *ASM International Handbook Committee*. 1990, 78-105, 509-514.

[18] Şenel, L. Al-Si Döküm alaşımlarının sıkıştırma döküm yöntemi ile mikroyapı ve mekanik özelliklerinin geliştirilmesi. Yüksek Lisans Tezi. Gazi Üniversitesi Fen Bilimleri Enstitüsü, Ankara. 2004.

[19]ASM Handbook Volume 3, Alloy Phase Diagrams, Binary Alloy Phase Diagrams. *ASM International Handbook Committee*. 1992, 279,337.

[20] Ahmad, S. Grain Refinement Of Al4cuti Alloy With Zirconium, Scandium And Erbium. Karadeniz Technical University. The Graduate School of Natural and Applied Sciences Department of Metallurgy & Materials Engineering. Master Thesis. 2018, 71.

[21] Paz, J.F.H. Heat treatment and precipitation in A356 aluminum alloy. Phd Thesis. McGill University. Montreal. 2003.

[22] Taşar, B. Toz Metalürjisi Yöntemi İle Üretilen Bor Ve Nikel Katkili A356 Alaşiminin Mikroyapi Ve Mekanik Özelliklerinin İncelenmesi, Karabük Üniversitesi. Lisansüstü Eğitim Enstitüsü İmalat Mühendisliği Anabilim Dalı. Yüksek Lisans Tezi. 2021.

[23] Wang, Y.; Schmidt, V.; Senz, S.; Gösele, U. Epitaxial growth of silicon nanowires using an aluminium catalyst. *Nature Nanotechnology*. 2006, 1(3),186-189.

[24] Abdulwahab, M.; Madugu, I.A.; Yaro, S.A.; Hassan, S.B.; Popoola, A.P.I. Effects of multiple-step thermal ageing treatment on the hardness characteristics of A356.0-type Al–Si–Mg alloy. *Materials and Design*. 2011, 32, 1159–1166.

[25] Demir, M. Al-Si-Mg alaşımlarında Mg etkisi, Yüksek Lisans Tezi, Karabük Üniversitesi Fen Bilimleri Enstitüsü, Karabük. 2012, 12-102.

[26] Güneren, A. T6 Heat Treatment Optimization Of A356 Alloy. Dokuz Eylül University. Graduate School Of Natural And Applied Sciences. Master Thesis. 2019.

[27] Horovitz, C. Scandium: Its Occurrence, Chemistry Physics, Metallurgy, Biology and Technology, 1975, 18-49

https://doi.org/10.1016/B978-0-12-355850-3.50007-1

[28] Borisenko, L. Scandium, Its Geochemistry and Mineralogy. New York: Consultants Bureau. 1961

[29] Baroch, C. T. Scandium. In B. o. Mines, Mineral Facts and Problems. Washington: United States Government Printing Office. 1960, 717-720

[30] Altinsel, Y. Investigation Of The Pre-Concentration Possibility Of Scandium Ores, Middle East Technical University. Mining Engineering Department. 2018.

[31] Ahmad, Z. The properties and application of Scandium-reinforced aluminum. *JOM* 55 (2). 2003, 35–39.

[32] Tack, W.T.; Hansson, I.L. Aluminum alloys containing Scandium with zirconium additions, U.S. Patent No. 5, 1997, 620.652.

[33] Zakharov, V.V. Effect of Scandium on the structure and properties of aluminum alloys. *Met. Sci. Heat Treat*.2003, 45 (7–8), 246–253.

[34] Jia, Z.; J. Røyset, J.K.; Solberg, L.I.U. Qing, Formation of precipitates and recrystallization resistance in Al–Sc–Zr alloys, Trans. *Nonferrous Metals Soc*. Chin. 2012, 1866–1871.

[35] Rosalbino, F.; Delsante, S.; Borzone, G.; Scavino, G. Assessing the corrosion resistance of binary Al-Sc alloys in chloride-containing environment: corrosion resistance of binary Al-Sc alloys. *Mater. Corros*. 2017, 68 (4), 444–449.

[36] Chandrasekaran, C. Testing of Rubber Lining. Anticorrosive Rubber Lining. 2017, 165–172.

https://doi:10.1016/b978-0-323-44371-5.00019-0

[37] Valiev, R.Z.; Salimonenko, D.A.; Tsenev, N.K.; Berbon, P.B.; Langdon, T.G. Observations of high strain rate superplasticity in commercial aluminum alloys with ultrafine grain sizes. *Scr. Mater*. 1997, 37 (12), 1945–1950.

[38] Cai, B.; Li, W.; Zhou, W.; Li, J.; Li, Z.; Li, W.; High temperature creep behavior of Al-0.2 Sc-0.04Zr alloys. Tezhong Zhuzao Ji YouseHejin/*Special Cast.Nonferrous Alloys*. 2014, 34 (2), 113–115.

[39] Kawasaki, M.; Langdon, T.G. Review: achieving superplastic properties in ultrafine-grained materials at high temperatures. *J. Mater. Sci*. 2016, 51 (1), 19–32.

[40] Prukkanon, W.; Srisukhumbowornchai, N.; Limmaneevichitr, C. Modification of hypoeutectic Al–Si alloys with Scandium. *J. Alloys Compd*. 2009, 477 (1), 454–460.

[41] Mousavi, M.G.; Cross, C.E.; Grong, Ø. Effect of Scandiumand titanium–boron on grain refinement and hot cracking of aluminium alloy 7108. *Sci. Technol. Weld. Join.* 1999, 4 (6), 381–388.

[42] Saatçi, G. Çekme Testleri İçin Yeni Bir Yazilim Geliştirilmesi Ve Denenmesi, Gazi Üniversitesi Fen Bilimleri Enstitüsü, Makina Mühendisliği Anabilim Dali, Yüksek Lisans Tezi, 2014.

[43] Soy, M. Metalik Malzemelerin Oda Sicakliğinda Yapilan Çekme Testlerinde A Ve B Tipi Ölçüm Belirsizliklerinin Karşilaştirilmasi. Yildiz Teknik Üniversitesi Fen Bilimleri Enstitüsü Metalürji Ve Malzeme Mühendisliği Anabilim Dali Malzeme Programi. Yüksek Lisans Tezi. 2019.

[44] Kiraz, A. Yapay Zeka Destekli Sanal Laboratuvar Tasarimi: Çekme Deneyi Uygulamasi, Sakarya Üniversitesi Fen Bilimleri Enstitüsü, Doktora Tezi. 2014.

[45] https://slideplayer.com/slide/13851999/ (Accessed 18,10,2021)

[46] Mills, D. Chapter 1 - Introduction to Pneumatic Conveying and the Guide, *Pneumatic Conveying Design Guide* (Third Edition). 2016, 3-32.

[47] Nedoseka, A. Supplementary sections: Numerical techniques and tests for welded structures, *Fundamentals of Evaluation and Diagnostics of Welded Structures*. 2012, 479-558.

[48] Sundararajan, G.; Roy, M. Hardness Testing, *Encyclopedia of Materials: Science and Technology.* 2001, 3728-3736.

[49] Onur, G. Alüminyum Silisyum Magnezyum Döküm Alaşımlarının Yapı İncelemesi, Tez (Yüksek Lisans) - İstanbul Teknik Üniversitesi, Fen Bilimleri Enstitüsü. 2006. http://hdl.handle.net/11527/9103

[50] GmbH, Z. Co. Z100/SN3A Materials Testing Machine Instruction Manual. Germany. 2002, 2 - 30. Serial Number: 156285

[51] Srinivasarao, M. 5 - Recent Advances in Optical MicroScopy and its Application to the Characterization of Polymers, *Comprehensive Polymer Science and Supplements*. 1989, 163-196,

[52] Zhang, J.; Zhang, H.; Wu, J.; Zhang, J. Fuel Cell Degradation and Failure Analysis. *Pem Fuel Cell Testing and Diagnosis*. 2013, 283-335.

[53] Di GianfranceSco, A. Technologies for chemical analyses, microstructural and inspection investigations, Materials for Ultra-Supercritical and Advanced Ultra-Supercritical Power Plants. 2017, 197-245.

[54] Omidi, M.; Fatehinya, A.; Farahani, M.; Akbari, Z.; Shahmoradi, S.; Yazdian, F.; Tahriri, M. Moharam zadeh, K.; Tayebi, L.; Vashaee, D. 7 - Characterization of biomaterials, Biomaterials for Oral and Dental Tissue Engineering. 2017, 97-115.

[55] Pednekar, P. P.; Godiyal, S. C.; Jadhav, K. R.; Kadam, V. J. Chapter 23 -Mesoporous silica nanoparticles: a promising multifunctional drug delivery system, *Nanostructures for Cancer Therapy*. 2017, 593-621.

[56] Abraham, J.; Jose, B.; Jose, A.; Thomas, S. Characterization of green nanoparticles from plants. *Phytonanotechnology*. 2020, 21–39.

https://doi:10.1016/b978-0-12-822348-2.00002-4

[57] Wang, G. C. Slag processing. The Utilization of Slag in Civil Infrastructure Construction. 2016, 87–113. https://doi:10.1016/b978-0-08-100381-7.00005-7

[58] Yesilkir-Baydar, S.; Oztel, O. N.; Cakir-Koc, R.; Candayan, A. Evaluation techniques. Nanobiomaterials Science. *Development and Evaluation*. 2017, 211–232. https://doi:10.1016/b978-0-08-100963-5.00011-2

[59] Zhang, W-G.; He, L-J.; Li, P-J.; Ye, Y-C.; X. Feng, L.S. Novikov, Dynamic response and numerical simulation of Al−Sc and Al−Ti alloys under high-speed impact. Trans. *Nonferrous Met. Soc*. China. 2015, 25, 559−570.

[60] Lathabai, S.; Lloyd, P.G.; The effect of Scandium on the microstructure, mechanical properties and weldability of a cast Al–Mg alloy. *Acta Materialia.* 2002, 50, 4275-4292.

[61] Tzeng, Y.-C.; Wu, C.-T.; Bor, H.-Y.; Horng, J.-L.; Tsai, M.-L.; Lee, S.-L. Effects of Scandium addition on iron-bearing phases and tensile properties of Al–7Si–0.6Mg alloys. *Materials Science and Engineering: A.* 2014, 593, 103–110. https://doi:10.1016/j.msea.2013.11.039

[62] Lim, Y. P.; Yeo, W. H.; Masita, A. The Effect of Scandium on the Mechanical Properties of A356 Aluminium Alloy. *Key Engineering Materials.* 2016, 707, 144–147. https://doi.org/10.4028/www.scientific.net/KEM.707.144

[63] Pramod, S. L.; Ravikirana, A. K.; Rao, P.; Murty, B. S.; Bakshi, S. R. Effect of Sc addition and T6 aging treatment on the microstructure modification and mechanical properties of A356 alloy. *Materials Science and Engineering: A.* 2016,674, 438–450.

https://doi: 10.1016/j.msea.2016.08.022

APPENDICES

APPENDIX A

Table A.1 Tensile test results

		Rod No	Yield Strenght (MPa)	Tensile Strength (MPa)	Elongation (%)	QI (MPa)
1	Reference	1	183.6	262.58	8.76	403.96
2	Reference	2	180.59	239.21	3.85	327.03
3	Reference	3	183.64	243.36	4.42	340.17
4	Reference	4	181.67	246.08	4.61	345.64
5	Reference	5	188.31	266.3	9.23	411.08
6	Reference	1	182.73	258.4	7.98	393.70
7	Reference	2	180.96	234.51	3.72	320.09
8	Reference	3	175.58	227.74	3.45	308.41
9	Reference	4	178.72	240.72	5	345.57
10	Reference	5	180.83	251.32	6.62	374.45
	AVERAGE		**181.663**	**247.022**	**5.764**	**357.0092**
1	0.2 wt.% Sc	1	180.03	259.3	8.87	401.49
2	0.2 wt.% Sc	2	177.76	249.65	6.99	376.32
3	0.2 wt.% Sc	3	183.3	248.02	5.73	361.74
4	0.2 wt.% Sc	4	178.58	255.89	7.37	386.01
5	0.2 wt.% Sc	5	185.26	266.72	11.47	425.65
6	0.2 wt.% Sc	1	181.35	260.71	8.78	402.23
7	0.2 wt.% Sc	2	180.93	253.75	6.89	379.48
8	0.2 wt.% Sc	3	180.32	254.56	7.07	381.97
9	0.2 wt.% Sc	4	183.08	256.68	7.6	388.80
10	0.2 wt.% Sc	5	179.5	265.86	10.7	420.2 7
	AVERAGE		**181.011**	**257.114**	**8.147**	**392.3978**
1	0.4 wt.% Sc	1	168.19	250.57	8.06	386.52
2	0.4 wt.% Sc	2	173.06	235.37	5.25	343.39
3	0.4 wt.% Sc	3	171.42	240.2 4	6.32	360.35
4	0.4 wt.% Sc	4	170.14	241.21	5.24	349.11
5	0.4 wt.% Sc	5	173.17	260.2 6	10.39	412.75
6	0.4 wt.% Sc	1	172.08	243.41	5.82	358.15
7	0.4 wt.% Sc	2	173.84	235.18	4.65	335.30
8	0.4 wt.% Sc	3	171.58	237.41	5.59	349.52

(cont. on next page)

Table A.1 (cont.)

9	0.4 wt.% Sc	4	176.1	247.36	6.9	373.19
10	0.4 wt.% Sc	5	175.29	260.12	9.41	406.16
	AVERAGE		**172.487**	**245.113**	**6.763**	**367.4438**
1	0.6 wt.% Sc	1	175.99	248.76	7.62	381.05
2	0.6 wt.% Sc	2	170.49	228.53	4.01	319.00
3	0.6 wt.% Sc	3	171.87	227.68	3.72	313.26
4	0.6 wt.% Sc	4	175.84	239.74	5.11	346.00
5	0.6 wt.% Sc	5	175.31	254.56	8.2	391.63
6	0.6 wt.% Sc	1	173.53	241.12	5.78	355.41
7	0.6 wt.% Sc	2	177.78	237.34	5.03	342.58
8	0.6 wt.% Sc	3	169.55	216.62	3.06	289.48
9	0.6 wt.% Sc	4	171.21	228.73	4.17	321.75
10	0.6 wt.% Sc	5	173.31	252.55	8.39	391.11
	AVERAGE		**173.488**	**237.563**	**5.509**	**345.1279**

APPENDIX B

Table B.1 Effect of %Sc on Hardness

Sample No	%Sc	Heat Treatment	Rod No	Yield Strength Rp 0.2 N/mm²	Tensile Strenght Rm N/mm²	Elongation %	Hardness (HB) 1. measurment	Hardness (HB) 2.measurment
Sc-01	Reference	Yes	1	183.6	262.58	8.76	80.38	75.33
			2	180.59	239.21	3.85		
			3	183.64	243.36	4.42		
			4	181.67	246.08	4.61		
			5	188.31	266.3	9.23		
			Average	183.56	251.51	6.17		
Sc-02	Reference	Yes	1	182.73	258.4	7.98	72.69	74.68
			2	180.96	234.51	3.72		
			3	175.58	227.74	3.45		
			4	178.72	240.72	5		
			5	180.83	251.32	6.62		
			Average	179.76	242.54	5.35		
	Reference	Yes	General Average	181.66	247.02	5.76	76.535	75.01
							75.77	
Sc-03	8 gr (0.2 %)	Yes	1	180.03	259.3	8.87	79.83	76.24

(cont. on next page)

Table B.1 (cont.)

			2	177.76	249.65	6.99		
			3	183.3	248.02	5.73		
			4	178.58	255.89	7.37		
			5	185.26	266.72	11.47		
			average	180.99	255.92	8.09		
Sc-04	8 gr (0.2 %)	Yes	1	181.35	260.71	8.78	75.34	77.74
			2	180.93	253.75	6.89		
			3	180.32	254.56	7.07		
			4	183.08	256.68	7.6		
			5	179.5	265.86	10.7		
			average	181.04	258.31	8.21		
	%0.2 wt. Sc	Yes	General Average.	181.01	257.11	8.15	77.585	76.99
							77.29	
Sc-05	16 gr (0.4 %)	Yes	1	168.19	250.57	8.06	76.8	68.47
			2	173.06	235.37	5.25		
			3	171.42	240.2 4	6.32		
			4	170.14	241.21	5.24		
			5	173.17	260.2 6	10.39		
			average	171.20	245.53	7.05		

(cont. on next page)

Table B.1 (cont.)

Sc-06	16 gr (0.4 %)	Yes	1	172.08	243.41	5.82	75.81	72.08
			2	173.84	235.18	4.65		
			3	171.58	237.41	5.59		
			4	176.1	247.36	6.9		
			5	175.29	260.12	9.41		
			average	173.78	244.70	6.47		
	%0.4 wt. Sc	Yes	General average	172.49	245.11	6.76	76.305	70.2 8
							73.29	
Sc-07	24 gr (0.6 %)	Yes	1	175.99	248.76	7.62	75.02	78.13
			2	170.49	228.53	4.01		
			3	171.87	227.68	3.72		
			4	175.84	239.74	5.11		
			5	175.31	254.56	8.2		
			average	173.90	239.85	5.73		
Sc-08	24 gr (0.6 %)	Yes	1	173.53	241.12	5.78	72.68	71.73
			2	177.78	237.34	5.03		
			3	169.55	216.62	3.06		
			4	171.21	228.73	4.17		
			5	173.31	252.55	8.39		
			average	173.08	235.27	5.29		
	%0.6 wt. Sc	Yes	General average	173.49	237.56	5.51	73.85	74.93
							74.39	

APPENDIX C

Table C.1 Represent Average Grain Size of each sample

Sample No	Alloy	Average Grain Size (micrometer)	Standard Deviation	Percentage of grain size by reference
Reference	A356	663.6	74.5	-
Sc2	A356	755.9	81.6	12.22%
Sc3	A356 - 0.2 wt.% Sc	662.4	64.9	-14.13%
Sc4	A356 - 0.2 wt.% Sc	680.6	70.5	2.69%
Sc5	A356 - 0.4 wt.% Sc	684.8	61.4	0.60%
Sc6	A356 - 0.4 wt.% Sc	864.8	104.4	20.82%
Sc7	A356 - 0.6 wt.% Sc	802.6	183.2	-7.75%
Sc8	A356 - 0.6 wt.% Sc	697.6	84.4	-15.05%